Molecular Pharmacology Fast Forward. Published on September 20, 2010 as doi:10.1124/mol.110.066332

The tarantula toxins ProTx-II and HWTX-IV differentially interact with human $Na_v1.7$ voltage-sensors to inhibit channel activation and inactivation

Yucheng Xiao, Kenneth Blumenthal, James O. Jackson II, Songping Liang and Theodore R. Cummins

Department of Pharmacology and Toxicology, Indiana University School of Medicine, Indianapolis, Indiana 46202 (Y.X., J.O.J., T.R.C.),

Department of Biochemistry, School of Medicine and Biomedical Sciences, State University of New York, Buffalo, New York 14214, USA (K.B.)

and

Key Laboratory of Protein Chemistry and Developmental Biology of the Ministry of Education, College of Life Sciences, Hunan Normal University, Changsha, Hunan 410081, China (Y.X., S. L.)

Molecular Pharmacology Fast Forward. Published on September 20, 2010 as DOI: 10.1124/mol.110.066332
This article has not been copyedited and formatted. The final version may differ from this version.

Running title: Inhibition of $hNa_v1.7$ gating by tarantula toxins

Corresponding author: Dr. Theodore R. Cummins, Department of Pharmacology and Toxicology, Stark Neurosciences Research Institute, Indiana University School of Medicine, Indianapolis, Indiana 46202, USA. Email: trcummin@iupui.edu.

Number of Text Pages: 33

Number of Tables: 2

Number of Figures: 7

Number of References: 32

Number of Words in Abstract: 248

Number of Words in Introduction: 580

Number of Words in Discussion: 1555

Abbreviations:

HWTX-IV, huwentoxin-IV; TTX, tetrodotoxin; Na_v, voltage-gated sodium channel; WT, wild type; HEK293, human embryonic kidney 293; domains I-IV, DI-DIV; transmembrane segments 1-6, S1-S6

Molecular Pharmacology Fast Forward. Published on September 20, 2010 as DOI: 10.1124/mol.110.066332
This article has not been copyedited and formatted. The final version may differ from this version.

Abstract

The voltage-gated sodium channel $Na_v1.7$ plays a crucial role in pain, and drugs that inhibit $hNa_v1.7$ may have tremendous therapeutic potential. ProTx-II and huwentoxin-IV (HWTX-IV), cystine knot peptides from tarantula venoms, preferentially block $hNa_v1.7$. Understanding the interactions of these toxins with sodium channels could aid the development of novel pain therapeutics. While both ProTx-II and HWTX-IV have been proposed to preferentially block $hNa_v1.7$ activation by trapping the domain-II voltage-sensor in the resting configuration, we show that specific residues in the voltage-sensor paddle of domain-II play substantially different roles in determining the affinities of these toxins to $hNa_v1.7$. The mutation E818C increases ProTx-II's and HWTX-IV's IC_{50} for block of $hNa_v1.7$ currents by 4- and 400-fold, respectively. In contrast, the mutation F813G decreases ProTx-II affinity by 9-fold, but has no effect on HWTX-IV affinity. Importantly, we also show that ProTx-II, but not HWTX-IV, preferentially interacts with $hNa_v1.7$ to impede fast-inactivation by trapping the domain-IV voltage-sensor in the resting configuration. Mutations E1589Q and T1590K in domain-IV each decreased ProTx-II's IC_{50} for impairment of fast-inactivation by ~6-fold. In contrast mutations D1586A and F1592A in domain-IV increased ProTx-II's IC_{50} for impairment of fast-inactivation by ~4-fold. Our results show that 1) while ProTx-II and HWTX-IV binding determinants on domain-II may overlap, domain-II plays a much more crucial role for HWTX-IV and 2) contrary to what has been proposed to be a guiding principle of sodium channel pharmacology, molecules do not have to exclusively target the domain-IV voltage-sensor in order to influence sodium channel inactivation.

Molecular Pharmacology Fast Forward. Published on September 20, 2010 as DOI: 10.1124/mol.110.066332
This article has not been copyedited and formatted. The final version may differ from this version.

Introduction

Voltage-gated sodium channels play important roles in action potential generation and propagation. As $Na_v1.7$ is a crucial contributor to pain sensation (Cox et al., 2006; Cummins et al., 2007), drugs that selectively target human $Na_v1.7$ ($hNa_v1.7$) could be ideal analgesics. Unfortunately drugs targeting sodium channels typically have broad spectrum sodium channel activity and narrow therapeutic windows (Cummins and Rush, 2007). Therefore there is substantial interest in identifying compounds that selectively target $hNa_v1.7$ and determining their molecular mechanisms of action.

ProTx-II and Huwentoxin-IV (HWTX-IV) are tarantula toxins that target voltage-gated sodium channels. These toxins belong to the inhibitory cystine knot family and are stabilized by the same disulfide frame (C1-C4, C2-C5 and C3-C6) (Middleton et al., 2002; Peng et al., 2002). However they show limited sequence similarity (Fig. 1A). Although ProTx-II inhibits multiple sodium channel subtypes ($Na_v1.1$-1.8), it has been reported to be ~100-fold more selective for $Na_v1.7$ (Schmalhofer et al., 2008; Smith et al., 2007). HWTX-IV preferentially inhibits tetrodotoxin (TTX)-sensitive neuronal subtypes (including $Na_v1.7$), does not inhibit TTX-resistant neuronal subtypes, and has little effect on skeletal muscle ($Na_v1.4$) and cardiac ($Na_v1.5$) subtypes (Xiao et al., 2008). Although these toxins have divergent properties, both are classified as voltage-sensor modifiers (Sokolov et al., 2008; Xiao et al., 2008).

Voltage-sensor modifiers target the voltage sensors of ion channels. The pore-forming sodium channel α-subunit consists of four domains (DI - DIV), each having six transmembrane segments (S1-S6) (Catterall et al., 2003). The S5-S6 segments form the channel pore and the S1-S4 segments form voltage sensor modules. The S4 segments, rich in positive residues, sense membrane depolarization and move outward to induce channel gating. Scorpion toxins have been extensively characterized as voltage-sensor modifiers, and understanding the molecular determinants of their interactions with voltage-gated sodium channels has provided invaluable insight into channel structure-function relationships. Scorpion α-toxins

Molecular Pharmacology Fast Forward. Published on September 20, 2010 as DOI: 10.1124/mol.110.066332
This article has not been copyedited and formatted. The final version may differ from this version.

interact with the DIV S3-S4 linker to stabilize DIV-S4 in the closed state, impeding fast inactivation. Scorpion β-toxins bind to the DII S3-S4 linker, trapping the DII-S4 in the activated state and enhancing channel activation. The binding sites for these scorpion toxins are defined as neurotoxin receptor sites 3 and 4, respectively (Cestele and Catterall, 2000). These data, in conjunction with other studies, indicate that the S4 segments in DI, DII and DIII are determinants of channel activation while that of DIV is predominantly involved in channel inactivation (Cestele et al., 2001; Cha et al., 1999; Sheets and Hanck, 2007). Both ProTx-II and HWTX-IV have been proposed to inhibit activation by trapping the DII voltage-sensor in the resting configuration. However, their binding determinants may not be identical. While HWTX-IV may selectively bind to neurotoxin site 4 (Xiao et al., 2008), ProTx-II may interact with novel binding sites on $Na_v1.5$ (Smith et al., 2007). Recently it was suggested that ProTx-II inhibits activation of $rNa_v1.2a$ by interacting with the voltage-sensor "paddles" (S3b-S4 motifs) of DI, DII and DIV (Bosmans et al., 2008). This finding was somewhat surprising given the presumed role of DIV in inactivation, leading to the proposal that for a toxin to alter inactivation it must exclusively interact with the voltage-sensor paddle of DIV (Bosmans et al., 2008).

We investigated the interactions of ProTx-II and HWTX-IV with the voltage-sensor paddles in $hNa_v1.7$ DI, DII and DIV. Our data show that these two tarantula toxins differ substantially in their interactions with $hNa_v1.7$. Although they may not be ideal as analgesic drugs, understanding the molecular determinants of their complicated interactions with voltage-gated sodium channels should aid the development of novel $hNa_v1.7$ blockers.

Molecular Pharmacology Fast Forward. Published on September 20, 2010 as DOI: 10.1124/mol.110.066332
This article has not been copyedited and formatted. The final version may differ from this version.

Materials and Methods

Toxins - ProTx-II was recombinantly produced as described by Smith et al. (Smith et al., 2007). HWTX-IV was purified from the crude venom of the female tarantula *O. huwena* as described by Peng *et al*. (Peng et al., 2002). The purity of ProTx-II and HWTX-IV was determined to be over 99% by high pressure liquid chromatography and matrix-assisted laser desorption ionization time-of-flight analysis.

Plasmids of sodium channels - The cDNA genes encoding rat (r) $Na_v1.2$, $rNa_v1.3$ and $rNa_v1.4$ were inserted into the vectors pRC-CMV, pcDNA3.1-mod and pRBG4, respectively (Cummins et al., 2001; O'Leary, 1998; Ukomadu et al., 1992). The cDNA genes encoding human (h) $Na_v1.5$ and $hNa_v1.7$ were subcloned into the vectors pcDNA3.1 and pcDNA3.1-mod, respectively (Klugbauer et al., 1995). Auxiliary subunits hβ1 and hβ2 were inserted into an internal ribosome entry site vector (Lossin et al., 2002).

Site-directed mutagenesis of $Na_v1.7$ - All $hNa_v1.7$ mutations in this study were constructed using the QuikChange II XL Site-Directed Mutagenesis kit according to the manufacture's instruction. All constructs were sequenced to confirm that the appropriate mutations were made.

Transient Transfection - Transient transfections of $hNa_v1.7$ wild type (WT) and mutant constructs into human embryonic kidney 293 (HEK293) cells were performed using the calcium phosphate precipitation method. HEK293 cells were grown under standard tissue culture conditions (5% CO_2 and 37 °C) in Dulbecco's modified Eagle's medium supplemented with 10% fetal bovine serum. The WT and mutant $hNa_v1.7$ channels were cotransfected with the hβ1 and hβ2 subunits to increase the current density. The calcium phosphate-DNA mixture (channel constructs and a green fluorescent protein reporter plasmid) was added to the cell culture medium and left for 3 h, after which the cells were washed with fresh medium. Cells with green fluorescent protein fluorescence were selected for whole-cell patch clamp

Molecular Pharmacology Fast Forward. Published on September 20, 2010 as DOI: 10.1124/mol.110.066332
This article has not been copyedited and formatted. The final version may differ from this version.

recordings 36-72 h after transfection. Stably transfected cell lines containing WT $rNa_v1.2$, $rNa_v1.3$, $rNa_v1.4$ and $hNa_v1.5$ without any β subunit or green fluorescent protein reporter plasmid were prepared using the method described previously (Xiao et al., 2008).

Whole-cell Patch Clamp Recordings - Whole-cell patch clamp recordings were carried out at room temperature (~21 °C) using an EPC-10 amplifier (HEKA, Lambrecht, Germany). Data were acquired on a Pentium IV computer using the Pulse program (version 8.31; HEKA). Fire-polished electrodes were fabricated from 1.7-mm capillary glass (VWR, West Chester, PA) using a P-97 puller (Sutter, Novato, CA). The standard pipette solution contained (in mM): 140 CsF, 1 EGTA, 10 NaCl and 10 HEPES, pH 7.3. The standard bathing solution was (in mM) 140 NaCl, 3 KCl, 1 MgCl2, 1 CaCl2 and 10 HEPES, pH 7.3. After filling with pipette solution, the access resistance of electrode pipette ranged from 0.8 to 1.4 MΩ and the average resistance was 0.98 ± 0.02 MΩ (n=250). The liquid junction potential for these solutions was <8 mV; data were not corrected to account for this offset. The offset potential was zeroed before contacting the cell. After establishing the whole-cell recording configuration, the resting potential was held at -100 mV for 5 min to allow adequate equilibration between the micropipette solution and the cell interior. Linear leak subtraction, based on resistance estimates from four to five hyperpolarizing pulses applied before the depolarizing test potential, was used for all voltage clamp recordings. Membrane currents were usually filtered at 5 kHz and sampled at 20 kHz. Voltage errors were minimized using 80% series resistance compensation, and the capacitance artifact was canceled using the computer-controlled circuitry of the patch clamp amplifier. The stock solutions for ProTx-II and HWTX-IV were made at 1 mM using bathing solution containing 1 mg/ml BSA, and aliquots were stored at -20 °C. Before use, the solution was diluted to the concentrations of interest with fresh bathing solution. Toxin was diluted into the recording chamber (volume of 300 µl) and mixed by repeatedly pipetting 30 µl to achieve the specified final concentration. The extent of the inhibitory effect of toxin was typically assessed around 10 - 20 min after toxin treatment.

Molecular Pharmacology Fast Forward. Published on September 20, 2010 as DOI: 10.1124/mol.110.066332
This article has not been copyedited and formatted. The final version may differ from this version.

Data Analysis - Data were analyzed using the Pulsefit (HEKA) and GraphPad Prism 4 (GraphPad Software) programs. All data points are shown as mean ± S.E. and *n* is presented as the number of the separate experimental cells. Steady-state activation and inactivation curves were fitted using Boltzmann equation: $y = 1/(1+\exp((V_{1/2}-V)/k)$, in which $V_{1/2}$, V and k represented midpoint voltage of kinetics, test potential and slope factor, respectively. Concentration-response curves to determine IC_{50} values were fitted using the Hill equation: $y = f_{bottom}(1- f_{bottom})/(1+([Tx]/IC_{50})^{nH})$, where *nH* is Hill coefficient, IC_{50} is half maximal inhibitory concentration, and f_{bottom} is the fraction of current resistant to inhibition at high toxin (Tx) concentration. For HWTX-IV, the *nH* was set to 1 because our mutagenesis data have shown that the toxin had a single high affinity binding site in $hNa_v1.7$. For ProTx-II slowing fast-inactivation, the *nH* was also set to 1 because only sodium channel DIV is involved in channel inactivation gating.

Molecular Pharmacology Fast Forward. Published on September 20, 2010 as DOI: 10.1124/mol.110.066332
This article has not been copyedited and formatted. The final version may differ from this version.

Results

ProTx-II and HWTX-IV block hNa$_v$1.7 channels at nanomolar concentrations. Although ProTx-II and HWTX-IV have previously been tested against hNa$_v$1.7 channels (Schmalhofer et al., 2008; Xiao et al., 2008), their activity has not been directly compared. Therefore we first compared the effects of ProTx-II and HWTX-IV on wild-type (WT) hNa$_v$1.7 channels expressed in HEK293 cells using whole cell voltage-clamp recordings. Although both toxins blocked the peak transient sodium currents conducted by hNa$_v$1.7, ProTx-II exhibited a 30-fold higher affinity for WT hNa$_v$1.7 than did HWTX-IV (Fig. 1D). The IC_{50} values for ProTx-II and HWTX-IV were determined to be 0.7 and 22.7 nM, respectively. Consistent with previous findings (Schmalhofer et al., 2008; Smith et al., 2007), 100 nM ProTx-II not only shifted channel activation in the depolarizing direction by 31.1 mV, but also increased the slope factor by twofold. In contrast, in the presence of 100 nM HWTX-IV, neither the activation nor the slope factor was obviously modified in the range of voltages tested in the present study (Fig. 1BC and Table 1-2). Because 100 nM is not a saturating concentration of HWTX-IV, it is likely that the residual currents shown in Fig. 1B result from channels that did not bind HWTX-IV. Indeed, in our previous study we showed that saturating concentrations of HWTX-IV shift the voltage-dependence of activation by at least 200 mV in the depolarizing direction (Xiao et al., 2008).

Comparison of the electrophysiological properties of WT and mutant hNa$_v$1.7 channels. To explore the molecular determinants of ProTx-II and HWTX-IV interactions with hNa$_v$1.7, we made specific mutations in the S3-S4 regions of DI, DII and DIV. We mainly focused on residues in the S3-S4 regions that previous studies have indicated were important for the inhibitory activity of either ProTx-II or HWTX-IV. The electrophysiological properties of mutant channels, expressed in HEK293 cells, were characterized under the whole-cell recording configuration and the voltage-dependent properties were compared to WT hNa$_v$1.7. The electrophysiological parameters of activation and steady-state inactivation, estimated by fitting the data with Boltzmann equations, are summarized in Supplemental Table S1. These

Molecular Pharmacology Fast Forward. Published on September 20, 2010 as DOI: 10.1124/mol.110.066332
This article has not been copyedited and formatted. The final version may differ from this version.

data indicate that acidic residues in extracellular S3-S4 linkers of DI and DII can modulate voltage-dependent activation of $hNa_v1.7$. Although the mutations L201V/N206D, F813G and F204A/F813G shifted the midpoint potentials of activation of $hNa_v1.7$ by less than +5 mV, the mutations of acidic residues E203K/E818C, E818C and F813G/E818C shifted activation by +17.6, +9.8 and +9.2 mV, respectively. This finding is consistent with previous reports that voltage sensors of DI and DII are important for channel activation (Cestele et al., 2001; Cha et al., 1999). By contrast, consistent with the finding that DIVS4 is mainly responsible for fast-inactivation (Cestele et al., 2001; Sheets and Hanck, 2007), mutations of most residues (D1586A, D1586E, E1589Q, T1590K, F1592A, and D1586A/T1590K) in DIV had limited effect on channel activation. Only the double mutation T1590K/F1592A substantially shifted channel activation, by +8.2 mV (Supplemental Table S1). None of mutations significantly altered steady-state inactivation. The slope factors for steady-state activation and inactivation also did not change compared to WT $hNa_v1.7$ (Supplemental Table S1).

Because the inhibition of $hNa_v1.7$ by ProTx-II is voltage dependent in the range of physiological voltages (Smith et al., 2007), the shifting of the current-voltage relationship caused by channel mutation might affect the assessment of toxin affinity when measured at the same test pulse potential. To precisely measure toxin affinity under similar activation conditions, the test pulse potential to activate $hNa_v1.7$ WT and mutant construct channels was set between -10 and +10 mV for the various constructs to ensure that ~90% channel conductance was available.

Mutations in DIIS3-S4 linker differentially decreased toxin affinities for $hNa_v1.7$. In previous studies, two residues in the DIIS3-S4 linker, F813 and E818 (Supplemental Fig. S1C), were shown to be important for $hNa_v1.7$ block by ProTx-II and HWTX-IV, respectively (Schmalhofer et al., 2008; Xiao et al., 2008). However, it is not known if F813 is important for HWTX-IV block or if E818 is important for ProTx-II block of $hNa_v1.7$. To determine whether these two tarantula toxins share the same binding site on the DIIS3-S4 linker of $hNa_v1.7$, we measured the IC_{50} values of the two toxins on two single

Molecular Pharmacology Fast Forward. Published on September 20, 2010 as DOI: 10.1124/mol.110.066332
This article has not been copyedited and formatted. The final version may differ from this version.

mutations, F813G and E818C using the whole-cell patch-clamp technique. As shown in Fig. 2, the F813G mutation decreased ProTx-II affinity for $hNa_v1.7$ by 9-fold with the IC_{50} value estimated to be 6.0 nM, but the value of HWTX-IV (28.2 nM) for this mutant was close to that (22.7 nM) for WT channels (see Tables 1 and 2). This result indicates that the residue F813 in $hNa_v1.7$ might interact structurally with ProTx-II but not HWTX-IV. Our previous work demonstrated that the neutralizing mutation E818Q could decrease HWTX-IV affinity by 63-fold (Xiao et al., 2008). Interestingly, when this acidic residue was substituted with Cys (E818C) in our present study, $hNa_v1.7$ current became substantially more resistant to HWTX-IV. Even when exposed to the toxin at concentrations up to 10 μM, $hNa_v1.7$-E818C current was only inhibited by 50.3 ± 3.0% (n = 3). The IC_{50} value was estimated to be 9.1 μM (Fig. 2B and Table 2), indicating that the E818C mutation decreased the sensitivity of $hNa_v1.7$ to HWTX-IV by at least 400-fold. By contrast, this mutation was found to only decrease ProTx-II affinity by 4-fold, with an IC_{50} value of 2.9 nM (Table 1). Given the weak decrease of ProTx-II block by E818C and the proximity of F813 to E818, it is possible that the decrease caused by the E818C mutation results from a change in the orientation of F813 within the DIIS3-S4 linker. To further examine this possibility, we constructed a double mutant F813G/E818C. The IC_{50} value of ProTx-II for the double mutant was estimated to be 29.8 nM in Fig. 2A (see Table 1). The decrease in ProTx-II affinity (42-fold) for the double mutant F813G/E818C is additive relative to the effects of the two single mutations from which it derived. Overall, these data strongly indicate that although the binding determinants of ProTx-II and HWTX-IV may partially overlap, they are not identical on $hNa_v1.7$ DII.

Mutations in DIS3-S4 linker did not significantly change toxin affinities for $hNa_v1.7$. As DII mutations only partially reduced ProTx-II block, and a previous study (Bosmans et al., 2008) showed that ProTx-II is likely to interact with multiple voltage sensors of $rNa_v1.2a$ including DI, we next asked if the extracellular DIS3-S4 linker contributes to the sensitivity of $hNa_v1.7$ for these two toxins. We first focused on E203 and F204 in DIS3-S4 of $hNa_v1.7$ (Supplemental Fig. S1C) because mutation of the corresponding residues in $rNa_v1.2a$ (E207 and F208) was reported to reduce the binding affinity of ProTx-

Molecular Pharmacology Fast Forward. Published on September 20, 2010 as DOI: 10.1124/mol.110.066332
This article has not been copyedited and formatted. The final version may differ from this version.

II for $rNa_v1.2a$ by 2.7- and 13.5-fold, respectively (Bosmans et al., 2008). Here we constructed two double mutants of $hNa_v1.7$ E203K/E818C and F204A/F813G, with the expectation that mutations that reduced binding at DII might help identify the contributions of residues in DI. The IC_{50} values of ProTx-II for E203K/E818C (4.6 nM) and F204A/F813G (8.2 nM) were not different from those of single mutants E818C (2.9 nM) and F813G (6.0 nM), respectively (Fig. 2A; Tables 1 and 2). These data suggested that although $hNa_v1.7$-E203 may have a weak interaction with ProTx-II, $hNa_v1.7$-F204 does not seem to play a role in ProTx-II inhibition of $hNa_v1.7$.

We were somewhat surprised that the E203K and F204A mutations did not significantly alter the effect of ProTx-II on $hNa_v1.7$, given the reported effect of the corresponding mutations on $rNa_v1.2a$. One possibility was that the difference between the relative impact of the DIS3-S4 substitutions in $rNa_v1.2a$ and $hNa_v1.7$ could be a result of overall sequence differences in the DIS3-S4 linker region. Although this linker region is highly conserved among voltage-gated sodium channel isoforms, $rNa_v1.2a$ differs from the $hNa_v1.7$ construct that we used at several positions in the DIS3-S4 linker. Interestingly, this linker is subject to alternative splicing in both $rNa_v1.2$ and $hNa_v1.7$ (Raymond et al., 2004). Splicing of exon 5 changes L201 and N206 (present in the variant that we have been testing) to Val and Asp in the D1S3-S4 linker, respectively (Chatelier et al., 2008). Sequence alignment shows that the V201 and D206 in the alternative splice variant $hNa_v1.7a$ are conserved at the corresponding positions in $rNa_v1.2a$ (V204 and D209) (see Supplemental Fig. S1). The effect of Ala-substitutions at these residues on $rNa_v1.2a$ sensitivity to ProTx-II was previously examined and, although the V204A mutation did not affect ProTx-II block of $rNa_v1.2a$/Kv2.1 chimeras, the D209A mutation decreased block in the chimeric channels by ~threefold (Bosmans et al., 2008). Therefore we examined if alternative splicing of DIS3-S4 of $hNa_v1.7$ could impact the sensitivity to ProTx-II. Fig. 2A shows that the IC_{50} value of ProTx-II was measured to be 1.0 nM for the variant $hNa_v1.7a$ (L201V/N206D), which is close to the value for WT $hNa_v1.7$. Although our results do not completely rule out the possibility that ProTx-II interacts with DIS3-S4 in $hNa_v1.7$, it indicates that such an interaction is less important than in $rNa_v1.2a$.

Molecular Pharmacology Fast Forward. Published on September 20, 2010 as DOI: 10.1124/mol.110.066332
This article has not been copyedited and formatted. The final version may differ from this version.

As shown in Fig. 2B, the concentration dependencies of HWTX-IV inhibition almost completely overlap for the mutants E818C and E203K/E818C, as did the curves for WT, F813G and F204A/F813G $Na_v1.7$ channels. Our data also indicate that alternative splicing of DIS3-S4 in $hNa_v1.7$ does not alter block by HWTX-IV (Fig. 2B and Table 1). Overall these data suggest that the DIS3-S4 linker is not a major determinant of either ProTx-II or HWTX-IV interactions with $hNa_v1.7$.

ProTx-II preferentially interacts with $hNa_v1.7$ to increase sustained currents. In the presence of 100 nM ProTx-II, 4.9 ± 0.6% of sodium channels could still be activated at -10 mV (Fig. 2A, n = 4). In an attempt to completely eliminate the $hNa_v1.7$ sodium current, we increased the ProTx-II concentration to 1 μM. However, no further block was observed, suggesting that the toxin effect on $hNa_v1.7$ activation saturates at a concentration of around 100 nM. Intriguingly, 1 μM ProTx-II was detected to significantly increase sustained currents generated by WT $hNa_v1.7$ (Fig. 3AB). The sustained currents did not decay completely during at least 50 ms. By contrast, in the presence of 1 (or even 10) μM HWTX-IV, no alternation of fast-inactivation of WT (or mutant E818C) $Na_v1.7$ channels was detected (see Supplemental Fig. S2). Since $hNa_v1.7$ currents induced at -10 mV inactivate completely within 10 ms in the absence of ProTx-II, we assayed the efficacy of toxin impeding fast-inactivation by measuring the $I_{10\ ms}/I_{peak}$ ratio, which gives an estimate of the probability for the channel to generate sustained currents after 10 ms. Sustained currents induced by 1 μM ProTx-II were detectable at voltages ranging from -40 to +70 mV, but at voltages more positive than +75 mV sustained currents were not evident (Fig. 3BD), indicating that the ProTx-II enhancement of sustained currents in $hNa_v1.7$ was voltage-dependent. Importantly, the sustained currents were blocked completely by 200 nM TTX, providing evidence that these sustained ionic currents were indeed fluxing through the $hNa_v1.7$ channel pore (Fig. 3CE).

We next wanted to estimate the concentration-response relationship of the apparent ProTx-II effect on the sustained current on multiple sodium channel subtypes expressed in HEK293 cells. Fig. 4A shows

Molecular Pharmacology Fast Forward. Published on September 20, 2010 as DOI: 10.1124/mol.110.066332
This article has not been copyedited and formatted. The final version may differ from this version.

representative current traces for five subtypes ($rNa_v1.2a$, $rNa_v1.3$, $rNa_v1.4$, $hNa_v1.5$ and $hNa_v1.7$) before and after application of 1 μM ProTx-II. As reported previously (Schmalhofer et al., 2008; Smith et al., 2007), the toxin IC_{50} for inhibition of activation of $hNa_v1.7$ was ~70-fold higher than for the other four subtypes $rNa_v1.2a$-$hNa_v1.5$ (Fig. 4B). In addition, while the sustained currents induced by 1 μM ProTx-II in $hNa_v1.7$ was 85.3 ± 3.4% of the peak current (n = 7), in $rNa_v1.2a$, $rNa_v1.3$, $rNa_v1.4$ and $hNa_v1.5$ it was only 18.0 ± 2.5%, 14.5 ± 1.1%, and 19.2 ± 4.0% (n = 3-4) of the peak current, respectively. As can be seen in Fig. 4C, fitting the data on the relative amplitude of the sustained currents induced by ProTx-II with the Hill equation yielded apparent IC_{50} values of 4.5, 5.6, 4.2, 4.1 and 0.24 μM for $rNa_v1.2a$, $rNa_v1.3$, $rNa_v1.4$, $hNa_v1.5$ and $hNa_v1.7$, respectively (Supplemental Table S2). It is difficult to accurately determine the IC_{50} values for apparent inhibition of inactivation. Comparisons of the apparent IC_{50} values are further complicated here because ProTx-II inhibits activation to different degrees for the different sodium channel isoforms. Despite these caveats, our data clearly indicate that ProTx-II preferentially induces sustained currents in $hNa_v1.7$ in addition to the preferential inhibition of $hNa_v1.7$ activation.

The voltage-dependent induction of sustained currents in $hNa_v1.7$ by ProTx-II is somewhat similar to the voltage-dependent inhibition of activation by ProTx-II. One explanation for the increased sustained currents is that ProTx-II might induce what appears to be sustained current by variably prolonging the latency to activation. However, the sustained currents are also similar to those induced by scorpion α-toxins that inhibit inactivation of voltage-gated sodium channels (Strichartz and Wang, 1986). Therefore an alternative explanation is that ProTx-II, in addition to its ability to inhibit activation, also inhibits inactivation, possibly by interacting with the $hNa_v1.7$ DIV voltage-sensor associated with inactivation in a manner similar to that of scorpion α-toxins (Rogers et al., 1996). Although all of the previous studies on ProTx-II have indicated that ProTx-II inhibits only activation of voltage-gated sodium channels (Bosmans et al., 2008; Middleton et al., 2002; Schmalhofer et al., 2008; Smith et al., 2007; Sokolov et al., 2008), Bosmans et al. reported that ProTx-II could interact with the DIV voltage sensor of $rNa_v1.2a$. Surprisingly, they found that specific substitutions in the S3-S4 linker region of DIV of $rNa_v1.2a$

Molecular Pharmacology Fast Forward. Published on September 20, 2010 as DOI: 10.1124/mol.110.066332
This article has not been copyedited and formatted. The final version may differ from this version.

substantially reduce the ability of ProTx-II to inhibit activation of $rNa_v1.2a$ channels expressed in *Xenopus* oocytes. Our results suggested that, at least for sodium channels expressed in mammalian cells, ProTx-II might be inducing sustained currents by interacting with DIV. If this effect is due to binding of DIV, the apparent affinity of ProTx-II binding for $hNa_v1.7$ DIV may be ~17-fold higher than for other subtypes.

Mutations in DIV alter ProTx-II's impact on sustained currents generated in $hNa_v1.7$. To further investigate how ProTx-II preferentially induced sustained sodium currents in $hNa_v1.7$, we compared the amino acid sequences of DIVS3-S4 linkers from eight sodium channel subtypes $Na_v1.1$-$Na_v1.8$ (Fig. 5). The most striking difference in this region is the unique presence of Thr-1590 in $hNa_v1.7$; the residue at the corresponding position in $rNa_v1.1$-$hNa_v1.6$ is Lys and Gln in $hNa_v1.8$. The residue at this position can be important in modulating the effect of scorpion α-toxins on sodium channels (Leipold et al., 2004). Importantly, D1586, E1589 and F1592 in $hNa_v1.7$ are conserved at the corresponding positions among six other subtypes ($Na_v1.1$-$Na_v1.6$). The residues at these positions are interesting as previous studies have determined that the first is crucial for the ability of site 3 scorpion α-toxins and sea anemone toxins to modify sodium channel inactivation and the latter two have been implicated in $rNa_v1.2a$ interactions with ProTx-II (Bosmans et al., 2008; Rogers et al., 1996). Therefore we next investigated if single substitutions at these four residues in $hNa_v1.7$ (D1586A, E1589Q, T1590K and F1592A) might be important determinants of ProTx-II preferentially inducing sustained currents in $hNa_v1.7$.

Current traces for these mutant channels were elicited by a 20-ms depolarizing potential of -10 or -5 mV from a holding potential of -100 mV (Fig. 6A). It is important to note that none of the four mutations altered the ability of ProTx-II to block $hNa_v1.7$ activation. As shown in Fig. 6B, the fit of the Hill equation yielded the IC_{50} values for ProTx-II inhibition of activation to be 1.0 nM (D1586A), 0.5 nM (E1589Q), 0.9 nM (T1590K) and 0.7 nM (F1592A). In contrast, these mutations had distinct effects on the ability of ProTx-II to induce $hNa_v1.7$ sustained currents (Fig. 6A and Supplemental Fig. S4). Two of

Molecular Pharmacology Fast Forward. Published on September 20, 2010 as DOI: 10.1124/mol.110.066332
This article has not been copyedited and formatted. The final version may differ from this version.

the mutations significantly decreased the enhancement of sustained currents by ProTx-II. The sustained currents induced by ProTx-II (1 μM) in E1589Q and T1590K channels were 40.3 ± 1.7% (n = 4) and 37.2 ± 10.0% (n = 3) of the peak current, respectively. The other two DIV mutations that we tested increased the ability of ProTx-II to enhance sustained currents. When treated only with 100 nM toxin, the sustained currents generated in D1586A and F1592A channels was 74.5 ± 2.6% (n = 4) and 61.1 ± 12.8% (n = 4) of the peak current, respectively, which are close to the value obtained for 1 μM ProTx-II on WT hNa$_v$1.7. As ProTx-II inhibits activation of the DIV mutant channels and WT channels to the same extent, we can confidently compare the relative effect on inhibition of inactivation by measuring the current amplitude 10 ms into the depolarizing pulse (I_{10ms}) and calculating the ratio (I_{10ms}/ I_{peak}), where I_{peak} is the peak current remaining after ProTx-II treatment. In Fig. 6C, the apparent IC$_{50}$ values for ProTx-II inhibition of fast-inactivation were estimated to be 48.3 nM, 1.6 μM, 1.4 μM, 70.1 nM and 240 nM for D1586A, E1589Q, T1590K, F1592A and WT hNa$_v$1.7, respectively (see Supplemental Table S2). Therefore, our data show that while two mutations E1589Q and T1590K selectively decreased ProTx-II ability to induce sustained currents in hNa$_v$1.7 DIV by ~6-fold, the other two mutations D1586A and F1592A selectively increased ProTx-II ability to induce sustained currents by ~4-fold.

These findings are very different from those of a previous study which found that the conserved mutations E1614A and F1620A in rNa$_v$1.2a decreased ProTx-II inhibition of rNa$_v$1.2a *activation* by over 6-fold and decreased ProTx-II affinity for the rNa$_v$1.2a DIV paddle motif by over 10-fold (Bosmans et al., 2008). Again in these previous studies, carried out with rNa$_v$1.2a, ProTx-II reportedly had no effect on sustained currents or inactivation. As can be seen in Fig. 5, there are only 2 differences in the DIVS3-S4 linkers of hNa$_v$1.7 and rNa$_v$1.2a: Asp-1586 and Thr-1590 of hNa$_v$1.7 are substituted with Glu and Lys, respectively, in rNa$_v$1.2a. When we replaced Asp-1586 with Glu in hNa$_v$1.7, the ability of ProTx-II to inhibit channel activation or induce sustained currents were not changed compared to WT channels (Fig. 6BC and Table 1), indicating that the sequence difference at this residue is not important in determining the differences between our observations and those of Bosmans et al. (2008). However, it has been clearly shown that

Molecular Pharmacology Fast Forward. Published on September 20, 2010 as DOI: 10.1124/mol.110.066332
This article has not been copyedited and formatted. The final version may differ from this version.

DIV residues can have substantial combinatorial effects on the interaction of scorpion α-toxins with specific sodium channel isoforms (Leipold et al., 2004). Therefore, we next asked whether the residue at position 1590 (Thr versus Lys) was the key factor for reversing the structural interactions of D1586 and F1592 with ProTx-II. Using the mutant T1590K as a model, we constructed two double mutations D1586A/T1590K and T1590K/F1592A. As seen in Fig. 7, the IC_{50} values for ProTx-II inducing sustained currents were estimated to be 0.26 μM for D1586A/T1590K and 0.18 μM for T1590K/F1592A, which were 5-fold and 7-fold smaller than the value for the single mutation T1590K, respectively (Supplemental Table S2). Therefore, together with the data on two single mutations D1586A and F1592A (Fig. 7C), these results suggest that the Thr to Lys exchange at position 1590 could not reverse the structural interaction of D1586 and F1592 with ProTx-II. In addition, neither double mutation altered the ability of ProTx-II to inhibit channel activation (Fig. 7B and see Table 1).

Finally, we asked whether decreasing the inhibition of action of $hNa_v1.7$ by ProTx-II would alter the apparent effects of ProTx-II on inactivation. Therefore we used the F813G/E818C double mutation, which reduces inhibition of activation by approximately 42-fold, and examined the impact of the E1589Q and F1592A mutations (Supplemental Fig. S5). In the F813G/E818C background, the E1589Q and F1592A mutations still have no effect on the inhibition of activation by ProTx-II, but the E1589Q mutation decreased the inhibition of inactivation by 5-fold and the F1592A mutation increased the inhibition of inactivation by 8-fold (Supplemental Fig. S5C). Thus these DIV mutations have nearly identical effects on ProTx-II inhibition of inactivation for WT and F813G/E818C mutant $Na_v1.7$ channels. Collectively, our data show that while mutations in DIV of $hNa_v1.7$ do not alter the inhibition of activation by ProTx-II, they do substantially modulate the ability of ProTx-II to induce sustained sodium currents in $hNa_v1.7$. This is similar to the DIV dependent inhibition of inactivation by scorpion α-toxins, indicating that ProTx-II can inhibit both activation *and* inactivation of voltage-gated sodium channels.

Molecular Pharmacology Fast Forward. Published on September 20, 2010 as DOI: 10.1124/mol.110.066332
This article has not been copyedited and formatted. The final version may differ from this version.

Discussion

We investigated the molecular determinants of the interactions of two tarantula toxins with $hNa_v1.7$. ProTx-II and HWTX-IV have a similar cysteine knot structure and both exhibit higher affinities for blocking $hNa_v1.7$ than for other subtypes (Schmalhofer et al., 2008; Xiao et al., 2008). However, these two toxins differ quite substantially in their non-cysteine sequence and our data indicate that they are very different in the extent and functional consequences of their interactions with $hNa_v1.7$.

Differential interactions of ProTx-II and HWTX-IV with $hNa_v1.7$ voltage-sensors. ProTx-II and HWTX-IV are classified as voltage-sensor modifiers and both have been proposed to selectively inhibit channel activation by trapping the DII voltage-sensor in the closed state (Sokolov et al., 2008; Xiao et al., 2008). Our results reveal that a single mutation (E818C) reduced the sensitivity of $hNa_v1.7$ for HWTX-IV by over 400-fold (Table 1). Our results further show that mutations of residues in the S3-S4 linkers of DI and DIV did not alter the inhibition of $hNa_v1.7$ by HWTX-IV. The DII voltage-sensor is clearly the main determinant of action for HWTX-IV inhibition of activation of $hNa_v1.7$.

In contrast, ProTx-II is likely to interact with multiple regions of sodium channels. In a study of ProTx-II interactions with $Na_v1.5$, we concluded that ProTx-II may not make critical interactions with extracellular linker regions of $Na_v1.5$, suggesting the existence of a novel toxin binding site (Smith et al., 2007). On the other hand, two studies with $rNa_v1.2a$ (Sokolov et al., 2008) and $hNa_v1.7$ (Schmalhofer et al., 2008) suggested that ProTx-II might specifically interact with the DII voltage-sensor. However, using chimeric Kv2.1 channels containing the voltage sensor paddle regions of $rNa_v1.2a$, Bosmans et al. (2008) found that ProTx-II can interact with the voltage sensors from three domains (DI, DII and DIV) of $rNa_v1.2a$. Consistent with this finding, we demonstrate that ProTx-II interacts with the voltage sensors of two domains (DII and DIV) in $hNa_v1.7$. However, our data suggest that the DIS3-S4 linker is less important in determining $hNa_v1.7$ sensitivity to ProTx-II than might be predicted by the chimeric paddle approach

Molecular Pharmacology Fast Forward. Published on September 20, 2010 as DOI: 10.1124/mol.110.066332
This article has not been copyedited and formatted. The final version may differ from this version.

and raises the possibility that other regions of the DI voltage-sensor (such as the S1-S2 linkers) may influence the isoform specific interactions.

The binding determinants of ProTx-II and HWTX-IV partially overlap on hNa$_v$1.7 DII. ProTx-II is at least 70-fold more selective for hNa$_v$1.7 over other subtypes that we tested, consistent with previous findings (Schmalhofer et al., 2008; Smith et al., 2007). Our data supports the assertion (Schmalhofer et al., 2008) that this selectivity might result from the higher sensitivity of hNa$_v$1.7 DII for ProTx-II. In DII, F813 is unique in hNa$_v$1.7. When F813 is substituted with Gly, the corresponding residue in most other sodium channel subtypes, we found that ProTx-II affinity for hNa$_v$1.7 is decreased by 9-fold. This decrease is smaller than that previously reported, where the F813G mutation completely abolished selectivity of ProTx-II for hNa$_v$1.7. It is not clear what accounts for this quantitative difference; however in the previous study the reverse substitution in hNa$_v$1.2 (G839F) did not significantly increase ProTx-II inhibition of hNa$_v$1.2 (Schmalhofer et al., 2008), indicating that the residue at this position is not the only determinant of hNa$_v$1.7's high sensitivity to ProTx-II. Interestingly, F813 is specific for ProTx-II's interaction and does not seem to play any role in HWTX-IV's interactions. Furthermore, we show that although E818 interacts with both toxins, it is much more important for HWTX-IV. Therefore our data indicate that the DIIS3-S4 linker is important in determining the higher selectivity of these toxins for hNa$_v$1.7, but the binding determinants of ProTx-II and HWTX-IV only partially overlap in this region. This observation, in combination with the striking lack of identity between ProTx-II and HWTX-IV, suggests that DII of hNa$_v$1.7 may be an excellent target for development of hNa$_v$1.7 specific inhibitors.

Molecular mechanism for ProTx-II inhibition of fast-inactivation. We observed that ProTx-II induced sustained hNa$_v$1.7 currents. Because ProTx-II dissociates from hNa$_v$1.7 at depolarized potentials, one explanation for the sustained current could have been that ProTx-II simply prolonged the latency to channel opening without any effect on inactivation. However, mutations in hNa$_v$1.7 DIV that substantially modulated the sustained current induced by ProTx-II had no effect on the inhibition of

Molecular Pharmacology Fast Forward. Published on September 20, 2010 as DOI: 10.1124/mol.110.066332
This article has not been copyedited and formatted. The final version may differ from this version.

activation by ProTx-II, in both the WT and F813G/E818C backgrounds. Interestingly, no effect was seen on the voltage-dependence of steady-state inactivation with ProTx-II (Fig. 1C); however, it should be noted that disparate effects on the voltage-dependence of steady-state inactivation and the rate of open-state fast-inactivation are frequently observed for DIV manipulations (Bendahhou et al., 1999; Yang et al., 1994). Scorpion α-toxins often have no effect on the voltage-dependence of steady-state fast-inactivation but dramatically inhibit open-state fast-inactivation of voltage-gated sodium channels (Maertens et al., 2006) and this action is dependent on the DIVS3-S4 linker (Rogers et al., 1996). Based on these previous studies and our data showing that the DIV mutations selectively alter the ability of ProTx-II to induce sustained currents in $hNa_v1.7$, we conclude that ProTx-II not only has the ability to inhibit activation, but also inhibits fast-inactivation of sodium channels through a mechanism similar to neurotoxin receptor site 3 toxins such as α-toxins.

Our data indicate that the effects on activation and inactivation are independent. Mutations in domain IV that substantially alter the effect on the inhibition of inactivation have no effect on the inhibition of activation. Mutations in domain II preferentially impact the inhibition of activation. This suggests that ProTx-II can simultaneously interact with two independent sites, one in DIV and the other possibly in DII. The estimated IC_{50} for inhibition of activation is ~400-fold smaller than the apparent IC_{50} for inhibition of inactivation, providing additional evidence that there are likely two independent interaction sites. Despite this differential in IC_{50}'s, the interaction with DIV is able to induce measurable sustained currents because the inhibition of activation is incomplete, even at relatively high concentrations.

These findings have some important implications. First, they point out potential limitations in the usefulness of ProTx-II as a research tool. Although ProTx-II may help determine if $Na_v1.7$ contributes to peak transient sodium currents in neurons, our results indicate that it would be problematic to use ProTx-II to determine the contribution of $Na_v1.7$ to sustained sodium currents. Second, it must also be used with care when examining the contribution of $Na_v1.7$ to action potential firing properties. Excitatory toxins

Molecular Pharmacology Fast Forward. Published on September 20, 2010 as DOI: 10.1124/mol.110.066332
This article has not been copyedited and formatted. The final version may differ from this version.

such as scorpion α-toxins and the tarantula toxin Jingzhaotoxin-I that impede fast-inactivation can prolong action potential duration and increase repetitive action potential firing (Rogers et al., 1996; Xiao et al., 2007; Xiao et al., 2005). Sustained $Na_v1.7$ currents induced by ProTx-II, even small ones, could be problematic. Sensory neurons that express $Na_v1.7$ often express other sodium channel isoforms such as $Na_v1.8$ that are less sensitive to ProTx-II (Middleton et al., 2002), and the persistent $Na_v1.7$ currents induced by ProTx-II in conjunction with $Na_v1.8$ currents could have complicated effects on excitability. The multiple effects of ProTx-II on $hNa_v1.7$ activation and inactivation would be expected to complicate, if not contraindicate, the use of ProTx-II administration to inhibit pain.

A previous report concluded that although ProTx-II interacts with the voltage-sensor paddles of DI, DII and DIV, ProTx-II only inhibited $rNa_v1.2a$ activation, not inactivation (Bosmans et al., 2008). As mutations in $rNa_v1.2a$ DI, DII *and* DIV paddles all affected the extent of inhibition of activation of $rNa_v1.2a$, it was concluded that drugs targeting any of the paddle motifs in the first three domains would only influence channel activation, regardless of any interaction with DIV. Furthermore, as DIV mutations altered the ability of ProTx-II to inhibit activation of $rNa_v1.2a$ channels expressed in *Xenopus* oocytes, it was concluded that toxins need to *exclusively* interact with the voltage-sensor of DIV in order to alter inactivation of voltage-gated sodium channels (Bosmans et al., 2008). Our results challenge the broad applicability of these conclusions. It is not entirely clear what accounts for the seemingly opposite actions of ProTx-II on the DIV's of $rNa_v1.2a$ and $hNa_v1.7$. We found that ProTx-II could impede fast-inactivation in multiple isoforms expressed in HEK293 cells, including $rNa_v1.2a$. Because the effects on fast-inactivation are much smaller in $rNa_v1.2a$, $rNa_v1.3$, $rNa_v1.4$ and $hNa_v1.5$ than in $hNa_v1.7$, they might have been overlooked in previous studies. Alternatively, the differential effects of ProTx-II could result from differences between *Xenopus* oocytes and mammalian cells. Differences in the lipid composition of the membrane could be a factor as ProTx-II exhibits substantial lipid binding activity (Smith et al., 2005). Indeed, the sensitivity of potassium channels to tarantula toxins can be modulated by differences in the

composition of the lipid bilayer (Schmidt and MacKinnon, 2008). Differences in posttranslational modifications, such as glycosylation, might also modulate the sensitivity of sodium channels to ProTx-II.

In summary, in this study we extensively investigated the interaction of two tarantula toxins with $hNa_v1.7$. HWTX-IV selectively inhibits activation of $hNa_v1.7$ and this is specifically determined by residues in the DII voltage sensor. ProTx-II also interacts with DII, but our data indicates that ProTx-II inhibits both activation and inactivation of $hNa_v1.7$. These data show that, contrary to what has previously been proposed to be a guiding principle of sodium channel pharmacology, toxins do not have to exclusively target the DIV voltage sensor in order to influence sodium channel inactivation. Molecules that interact with the multiple voltage-sensors of sodium channels can impede both activation and inactivation, and these complex interactions need to be carefully considered when targeting the voltage-sensors of sodium channels.

Molecular Pharmacology Fast Forward. Published on September 20, 2010 as DOI: 10.1124/mol.110.066332
This article has not been copyedited and formatted. The final version may differ from this version.

References

Bendahhou S, Cummins TR, Kwiecinski H, Waxman SG and Ptacek LJ (1999) Characterization of a new sodium channel mutation at arginine 1448 associated with moderate Paramyotonia congenita in humans. *J Physiol* **518 (Pt 2)**:337-344.

Bosmans F, Martin-Eauclaire MF and Swartz KJ (2008) Deconstructing voltage sensor function and pharmacology in sodium channels. *Nature* **456**:202-208.

Catterall WA, Goldin AL and Waxman SG (2003) International Union of Pharmacology. XXXIX. Compendium of voltage-gated ion channels: sodium channels. *Pharmacol Rev* **55**:575-578.

Cestele S and Catterall WA (2000) Molecular mechanisms of neurotoxin action on voltage-gated sodium channels. *Biochimie* **82**:883-892.

Cestele S, Scheuer T, Mantegazza M, Rochat H and Catterall WA (2001) Neutralization of gating charges in domain II of the sodium channel alpha subunit enhances voltage-sensor trapping by a beta-scorpion toxin. *J Gen Physiol* **118**:291-302.

Cha A, Ruben PC, George AL, Jr., Fujimoto E and Bezanilla F (1999) Voltage sensors in domains III and IV, but not I and II, are immobilized by Na+ channel fast inactivation. *Neuron* **22**:73-87.

Chatelier A, Dahllund L, Eriksson A, Krupp J and Chahine M (2008) Biophysical properties of human $Na_v1.7$ splice variants and their regulation by protein kinase A. *J Neurophysiol* **99**:2241-2250.

Cox JJ, Reimann F, Nicholas AK, Thornton G, Roberts E, Springell K, Karbani G, Jafri H, Mannan J, Raashid Y, Al-Gazali L, Hamamy H, Valente EM, Gorman S, Williams R, McHale DP, Wood JN, Gribble FM and Woods CG (2006) An SCN9A channelopathy causes congenital inability to experience pain. *Nature* **444**:894-898.

Cummins TR, Aglieco F, Renganathan M, Herzog RI, Dib-Hajj SD and Waxman SG (2001) $Na_v1.3$ sodium channels: rapid repriming and slow closed-state inactivation display quantitative differences after expression in a mammalian cell line and in spinal sensory neurons. *J Neurosci* **21**:5952-5961.

Cummins TR and Rush AM (2007) Voltage-gated sodium channel blockers for the treatment of neuropathic pain. *Expert Rev Neurother* **7**:1597-1612.

Cummins TR, Sheets PL and Waxman SG (2007) The roles of sodium channels in nociception: Implications for mechanisms of pain. *Pain* **131**:243-257.

Klugbauer N, Lacinova L, Flockerzi V and Hofmann F (1995) Structure and functional expression of a new member of the tetrodotoxin-sensitive voltage-activated sodium channel family from human neuroendocrine cells. *Embo J* **14**:1084-1090.

Leipold E, Lu S, Gordon D, Hansel A and Heinemann SH (2004) Combinatorial interaction of scorpion toxins Lqh-2, Lqh-3, and LqhalphaIT with sodium channel receptor sites-3. *Mol Pharmacol* **65**:685-691.

Lossin C, Wang DW, Rhodes TH, Vanoye CG and George AL, Jr. (2002) Molecular basis of an inherited epilepsy. *Neuron* **34**:877-884.

Maertens C, Cuypers E, Amininasab M, Jalali A, Vatanpour H and Tytgat J (2006) Potent modulation of the voltage-gated sodium channel $Na_v1.7$ by OD1, a toxin from the scorpion Odonthobuthus doriae. *Mol Pharmacol* **70**:405-414.

Middleton RE, Warren VA, Kraus RL, Hwang JC, Liu CJ, Dai G, Brochu RM, Kohler MG, Gao YD, Garsky VM, Bogusky MJ, Mehl JT, Cohen CJ and Smith MM (2002) Two tarantula peptides inhibit activation of multiple sodium channels. *Biochemistry* **41**:14734-14747.

O'Leary ME (1998) Characterization of the isoform-specific differences in the gating of neuronal and muscle sodium channels. *Can J Physiol Pharmacol* **76**:1041-1050.

Peng K, Shu Q, Liu Z and Liang S (2002) Function and solution structure of huwentoxin-IV, a potent neuronal tetrodotoxin (TTX)-sensitive sodium channel antagonist from Chinese bird spider Selenocosmia huwena. *J Biol Chem* **277**:47564-47571.

Raymond CK, Castle J, Garrett-Engele P, Armour CD, Kan Z, Tsinoremas N and Johnson JM (2004) Expression of alternatively spliced sodium channel alpha-subunit genes. Unique splicing patterns are observed in dorsal root ganglia. *J Biol Chem* **279**:46234-46241.

Rogers JC, Qu Y, Tanada TN, Scheuer T and Catterall WA (1996) Molecular determinants of high affinity binding of alpha-scorpion toxin and sea anemone toxin in the S3-S4 extracellular loop in domain IV of the Na+ channel alpha subunit. *J Biol Chem* **271**:15950-15962.

Schmalhofer WA, Calhoun J, Burrows R, Bailey T, Kohler MG, Weinglass AB, Kaczorowski GJ, Garcia ML, Koltzenburg M and Priest BT (2008) ProTx-II, a selective inhibitor of $Na_v1.7$ sodium channels, blocks action potential propagation in nociceptors. *Mol Pharmacol* **74**:1476-1484.

Schmidt D and MacKinnon R (2008) Voltage-dependent K+ channel gating and voltage sensor toxin sensitivity depend on the mechanical state of the lipid membrane. *Proc Natl Acad Sci U S A* **105**:19276-19281.

Sheets MF and Hanck DA (2007) Outward stabilization of the S4 segments in domains III and IV enhances lidocaine block of sodium channels. *J Physiol* **582**:317-334.

Smith JJ, Alphy S, Seibert AL and Blumenthal KM (2005) Differential phospholipid binding by site 3 and site 4 toxins. Implications for structural variability between voltage-sensitive sodium channel domains. *J Biol Chem* **280**:11127-11133.

Smith JJ, Cummins TR, Alphy S and Blumenthal KM (2007) Molecular interactions of the gating modifier toxin ProTx-II with NaV 1.5: implied existence of a novel toxin binding site coupled to activation. *J Biol Chem* **282**:12687-12697.

Sokolov S, Kraus RL, Scheuer T and Catterall WA (2008) Inhibition of sodium channel gating by trapping the domain II voltage sensor with protoxin II. *Mol Pharmacol* **73**:1020-1028.

Strichartz GR and Wang GK (1986) Rapid voltage-dependent dissociation of scorpion alpha-toxins coupled to Na channel inactivation in amphibian myelinated nerves. *J Gen Physiol* **88**:413-435.

Ukomadu C, Zhou J, Sigworth FJ and Agnew WS (1992) muI Na+ channels expressed transiently in human embryonic kidney cells: biochemical and biophysical properties. *Neuron* **8**:663-676.

Xiao Y, Bingham JP, Zhu W, Moczydlowski E, Liang S and Cummins TR (2008) Tarantula huwentoxin-IV inhibits neuronal sodium channels by binding to receptor site 4 and trapping the domain II voltage sensor in the closed configuration. *J Biol Chem* **283(40)**: 27300-27313

Xiao Y, Li J, Deng M, Dai C and Liang S (2007) Characterization of the excitatory mechanism induced by Jingzhaotoxin-I inhibiting sodium channel inactivation. *Toxicon* **50**:507-517.

Xiao Y, Tang J, Hu W, Xie J, Maertens C, Tytgat J and Liang S (2005) Jingzhaotoxin-I, a novel spider neurotoxin preferentially inhibiting cardiac sodium channel inactivation. *J Biol Chem* **280**:12069-12076.

Yang N, Ji S, Zhou M, Ptacek LJ, Barchi RL, Horn R and George AL, Jr. (1994) Sodium channel mutations in paramyotonia congenita exhibit similar biophysical phenotypes in vitro. *Proc Natl Acad Sci U S A* **91**:12785-12789.

Molecular Pharmacology Fast Forward. Published on September 20, 2010 as DOI: 10.1124/mol.110.066332
This article has not been copyedited and formatted. The final version may differ from this version.

Footnotes

This work was supported by National Institutes of Health grants [NS054642 and NS053422], the 973 Research Program of China [Contract 2010CB529800] and the Program for New Century Excellent Talents in University [Contract NCET-07-0279].

Molecular Pharmacology Fast Forward. Published on September 20, 2010 as DOI: 10.1124/mol.110.066332
This article has not been copyedited and formatted. The final version may differ from this version.

Legends for Figures

Figure 1. Effects of ProTx-II and HWTX-IV on WT $Na_v1.7$ expressed in HEK293 cells. (A), Sequence alignment of ProTx-II and HWTX-IV. Six conserved cysteines are identified by the encompassing rectangles in the sequence alignment. (B), Differential effects of two toxins on the current-voltage relationships of WT $Na_v1.7$. Cells were held at -100 mV. $Na_v1.7$ currents were elicited by 50-ms depolarization steps to various voltages ranging from -80 to +100 mV in 5-mV increments. Currents elicited before and after application of 100 nM ProTx-II (left panel) or 100 nM HWTX-IV (right panel) were normalized to the maximum amplitude of control peak current. (C), Effects of the two toxins on normalized steady-state activation and inactivation of WT $Na_v1.7$. Channel conductances before and after application of 100 nM ProTx-II or 100 nM HWTX-IV were calculated with the equation: G(V) = I/(V-Vrev), in which *I*, *V* and *Vrev* represented inward current elicited as described in (B), test potential and reversal potential, respectively. Data are plotted as a fraction of the maximum conductance. The voltage dependence of steady-state inactivation was estimated using a standard double-pulse protocol, in which a 20-ms depolarizing test potential of 0 mV followed a 500-ms prepulse at potentials that ranged from -130 to -10 mV with a 10-mV increment. Cells were held at -100 mV. All curves were fit with the Boltzmann equation as described under "Experimental Procedures". (D), concentration-dependent inhibition of WT $Na_v1.7$ by two toxins. Data points (mean ± S.E., each from 3 - 4 cells) were fit with the Hill equation as described under "Experimental Procedures". The values of IC_{50}, slope factor (*nH*) and f_{bottom} yielded were shown in Table 1 and Table 2.

Figure 2. Concentration-response inhibitory curves of ProTx-II (A) and HWTX-IV (B) on DI and DII mutant $Na_v1.7$ channels. Sodium current was induced at 5 s intervals by a 20-ms depolarization from a holding potential of -100 mV. The test pulse potentials to activate channels were set to -10 mV (WT and L201V/N206D), -5 mV (F204A/F813G, F204A/F813G, F813G, E1589Q), 0 mV (E818C and F813G/E818C) and +10 mV (E203K/E818C), respectively. The residual current after toxin treatment was plotted as fraction of the control current. Data points (mean ± S.E., each from 3 - 7 cells) were fit with a Hill equation as described under "Experimental Procedures". The values of IC_{50}, slope factor (*nH*) and f_{bottom} yielded are shown in Table 1 and Table 2.

Molecular Pharmacology Fast Forward. Published on September 20, 2010 as DOI: 10.1124/mol.110.066332
This article has not been copyedited and formatted. The final version may differ from this version.

Figure 3. ProTx-II significantly impeded fast inactivation of WT $Na_v1.7$ expressed in HEK293 cells. Cells were held at -100 mV. Families of current traces before (A) and after application of 1 μM ProTx-II (B) or 200 nM TTX (C) were induced by 50-ms depolarizing steps to various potentials ranging from -100 to +100 mV in 5-mV increments. (D) and (E), Effects of 1 μM ProTx-II (D) or 200 nM TTX (E) on the current-voltage (I-V) relationship of WT $Na_v1.7$. All currents induced before and after toxin treatment were plotted as fraction of the maximum amplitude of control peak current. The dotted line indicates the control I-V curve. The red filled circles indicate the peak I-V curves after application of 1 μM ProTx-II. I_{10ms} (blue open diamond) was shown as the current inactivated at 10 ms after application of 1 μM ProTx-II. (E), Effects of 200 nM TTX on the current-voltage (I-V) relationship of WT Nav1.7 sustained currents induced by ProTx-II. All currents induced before and after toxin treatment were plotted as fraction of the maximum amplitude of control peak current. The dotted line indicates the control I-V curve. The green open circles indicate the I-V curve after application of 200 nM TTX. I_{10ms} (blue open diamond) was shown as the current inactivated at 10 ms after application of 1 μM ProTx-II.

Figure 4. ProTx-II differentially inhibited both activation and inactivation of sodium channel subtypes expressed in HEK293 cells. Cells were held at -100 mV. (A), Currents through WT $Na_v1.2$, $Na_v1.3$, $Na_v1.4$ and $Na_v1.7$ were induced by a 20-ms depolarizing potential of -10 mV. $Na_v1.5$ current was elicited at -30 mV. The dotted lines show the residual current in the presence of 1 μM ProTx-II after normalization to the maximum amplitude of control current. (B), Concentration-response inhibitory curves of ProTx-II on the activation of five sodium channel subtypes ($Na_v1.2$, $Na_v1.3$, $Na_v1.4$, $Na_v1.5$ and $Na_v1.7$). The residual current after ProTx-II treatment was plotted as a fraction of control current. Data points (mean ± S.E., each from 3-7 cells) were fit with Hill equation as described under "Experimental Procedure". The IC50 values were estimated to be 52.9 ± 1.1 ($Na_v1.2a$), 109.9 ± 7.1 ($Na_v1.3$), 107.6 ± 7.7 ($Na_v1.4$) and 79.4 ± 40.7 ($Na_v1.5$) nM, respectively. The slope factor (*nH*) ranged from 0.9 to 1.1. (C), Concentration-response inhibitory curves of ProTx-II on the fast-inactivation of five sodium channel subtypes. The I_{10ms} was plotted as a fraction of the residual current after ProTx-II treatment. Inhibition of fast-inactivation increases the ratio of I_{10ms}/ I_{peak}. Data points (mean ± S.E., each from 3-7 cells) were

Molecular Pharmacology Fast Forward. Published on September 20, 2010 as DOI: 10.1124/mol.110.066332
This article has not been copyedited and formatted. The final version may differ from this version.

fit with Hill equation as described under "Experimental Procedure". The IC_{50} values were shown in Supplementary Table 2.

Figure 5. Amino acid sequence alignment of the DIV S3-S4 linkers of seven α subunit isoforms from human. (A), Crucial determinants of neurotoxin receptor 3 are located in the S3-S4 linker of sodium channel domain II. The positions of amino acid residues of interest are shaded in grey. (B), Schematic diagram of sodium channel α subunit. The voltage sensor (the 4^{th} segment) of each domain is shaded in gray and marked with "+ +". The amino acid sequence of DIV S3-S4 linker is shown in the square frame of (A) as indicated by arrows.

Figure 6. Mutations in DIV S3-S4 linker differentially alter the effect of ProTx-II on fast-inactivation of $hNa_v1.7$ channels expressed in HEK293 cells. (A) Representative current traces for five mutant (D1586A, D1586E, E1589Q, T1590K and F1592A) $hNa_v1.7$ channels. The test pulse potential was -10 mV (D1586A and D1586E) and -5 mV (E1589Q, T1590K and F1592A), respectively. Cells were held at -100 mV. The dotted line shows the residual current in the presence of 0.1 or 1 μM ProTx-II after normalization to the maximum amplitude of control current. (B), Concentration-response inhibitory curves of ProTx-II on the activation of WT and five mutant (D1586A, D1586E, E1589Q, T1590K and F1592A) $Na_v1.7$ channels. Residual current after toxin treatment was plotted as a fraction of control peak current amplitude. Data points (mean ± S.E., each from 3-6 cells) were fitted with Hill equation as described under "Experimental Procedure". The calculated values of IC_{50}, slope factor (*nH*) and f_{bottom} are shown in Table 1. (C), Concentration-response inhibitory curves of ProTx-II on fast-inactivation of WT and five mutant (D1586A, D1586E, E1589Q, T1590K and F1592A) $Na_v1.7$ channels. The I_{10ms} was plotted as a fraction of the residual current after ProTx-II treatment. Data points (mean ± S.E., each from 3-6 cells) were fitted with Hill equation as described under "Experimental Procedure".

Figure 7. Two mutations (D1586A and F1592A) enhanced the ProTx-II slowing fast-inactivation of $hNa_v1.7$ in the presence of K1590. (A) Representative current traces for two double mutant (D1586A/T1590K and T1590K/F1592A) $hNa_v1.7$ channels. The test pulse potential was -5 mV for D1586A/T1590K and 0 mV for T1590K/F1592A, respectively. Cells were held at -100 mV. The dotted lines show the residual current in the

Molecular Pharmacology Fast Forward. Published on September 20, 2010 as DOI: 10.1124/mol.110.066332
This article has not been copyedited and formatted. The final version may differ from this version.

presence of 1 μM ProTx-II after normalization to the maximum amplitude of control current. (B), Concentration-response inhibitory curves of ProTx-II on the activation of three mutant (T1590K, D1586A/T1590K and T1590K/F1592A) $Na_v1.7$ channels. Residual current after toxin treatment was plotted as a fraction of control peak current amplitude. The calculated values of IC_{50}, slope factor (*nH*) and f_{bottom} are shown in Table 1. (C), Concentration-response inhibitory curves of ProTx-II on fast-inactivation of three mutant (T1590K, D1586A/T1590K and T1590K/F1592A) $Na_v1.7$ channels. The I_{10ms} was plotted as a fraction of the residual current after ProTx-II treatment. The IC50 values are shown in Supplementary Table 2. In (B) and (C), data points (mean ± S.E., each from 3 - 4 cells) are fit with a Hill equation as described under "Experimental Procedure".

Molecular Pharmacology Fast Forward. Published on September 20, 2010 as DOI: 10.1124/mol.110.066332
This article has not been copyedited and formatted. The final version may differ from this version.

Table 1

Channel	Voltage dependence of activation						
	control		ProTx-II				
	$V_{1/2}$, mV	*k*, mV	$V_{1/2,}$ mV	*k*, mV	IC_{50}, nM	*nH*	f_{bottom}
$hNa_v1.7$	-41.5 ± 0.8	6.5 ± 0.7	-10.4 ± 0.9	14.5 ± 0.8	0.7 ± 0.2	1.1 ± 0.2	0.05 ± 0.02
L201V/N206D	-42.5 ± 0.4	5.3 ± 0.4	-12.1 ± 1.0	17.1 ± 0.9	1.0 ± 0.3	1.1 ± 0.2	0.03 ± 0.01
F813G	-39.6 ± 0.2	5.5 ± 0.2	-23.0 ± 2.7	18.7 ± 2.8	6.0 ± 2.1	1.0 ± 0.2	0.09 ± 0.04
E818C	-33.0 ± 1.2	8.1 ± 1.1	-0.6 ± 1.2	15.3 ± 1.1	2.9 ± 0.1	1.0 ± 0.1	0.13 ± 0.03
E203K/E818C	-14.2 ± 0.4	9.0 ± 0.4	14.2 ± 1.8	19.2 ± 1.5	4.6 ± 0.7	1.2 ± 0.2	0.16 ± 0.02
F204A/F813G	-41.1 ± 1.3	7.2 ± 1.1	-26.3 ± 1.2	14.9 ± 1.2	8.2 ± 1.1	1.3 ± 0.2	0.08 ± 0.03
F813G/E818C	-34.0 ± 1.2	8.1 ± 1.1	-20.5 ± 1.4	15.3 ± 1.3	29.8 ± 3.6	1.0 ± 0.2	0.10 ± 0.05
D1586A	-33.0 ± 0.8	7.5 ± 0.7	-7.1 ± 1.2	16.6 ± 1.1	1.0 ± 0.1	1.2 ± 0.4	0.08 ± 0.04
D1586E	-40.6 ± 0.7	7.0 ± 0.6	-13.6 ± 1.9	17.5 ± 1.9	0.4 ± 0.03	1.0 ± 0.2	0.09 ± 0.02
E1589Q	-40.0 ± 1.6	8.4 ± 1.4	-11.7 ± 1.9	17.2 ± 1.8	0.5 ± 0.1	1.0 ± 0.1	0.06 ± 0.02
T1590K	-44.2 ± 0.5	5.2 ± 0.4	-16.2 ± 0.8	14.0 ± 0.7	0.9 ± 0.4	1.1 ± 0.3	0.07 ± 0.04
F1592A	-34.1 ± 1.1	8.0 ± 0.9	-5.3 ± 2.1	19.3 ± 2.1	0.7 ± 0.3	1.1 ± 0.4	0.04 ± 0.04
D1586A/T1590K	-40.5 ± 0.3	6.9 ± 0.2	-2.5 ± 0.8	18.5 ± 0.8	0.7 ± 0.4	0.8 ± 0.4	0.04 ± 0.01
T1590K/F1592A	-35.1 ± 0.2	6.9 ± 0.2	-8.3 ± 2.6	25.2 ± 2.9	0.8 ± 0.4	1.1 ± 0.1	0.06 ± 0.01

Table 1 Characterization of activation of $hNa_v1.7$ mutants in the presence of 100 nM ProTx-II. Cells were held at -100 mV. Families of currents were induced by 50-ms depolarizing steps to various potential ranging from -80 to +40 mV. Recording currents from WT and mutant $Na_v1.7$ started at ~20 min after establishing whole cell configuration. All data come from 3-4 cells. The half-activation potential ($V_{1/2}$) and slope factor (*k*) were determined with Boltzmann fits. The values of IC_{50}, slope factor (*nH*) and f_{bottom} were determined with Hill equation in Fig. 2A, Fig. 6B and Fig. 7B.

Molecular Pharmacology Fast Forward. Published on September 20, 2010 as DOI: 10.1124/mol.110.066332
This article has not been copyedited and formatted. The final version may differ from this version.

Table 2

Channel	Voltage dependence of activation				
	control		HWTX-IV		
	$V_{1/2}$, mV	*k*, mV	$V_{1/2}$, mV	*k*, mV	IC_{50}, nM
$hNa_v1.7$	-38.8 ± 0.8	6.8 ± 0.7	-40.2 ± 0.7	7.3 ± 0.6	22.7 ± 6.3
L201V/N206D	-40.4 ± 1.3	7.9 ± 1.2	-36.7 ± 1.2	9.6 ± 1.1	20.8 ± 3.6
F813G	-32.7 ± 1.0	6.7 ± 0.9	-36.3 ± 1.4	8.0 ± 1.3	28.2 ± 5.7
E818C	-41.6 ± 0.8*	7.1 ± 0.7*	-39.7 ± 0.9*	8.9 ± 0.8*	9120.1 ± 1400.0
E203K/E818C	-20.5 ± 0.3*	8.5 ± 0.3*	-16.0 ± 1.1*	13.8 ± 1.0*	8892.0 ± 1135.2
F204A/F813G	-46.7 ± 0.4	4.5 ± 0.3	-42.7 ± 0.4	6.1 ± 0.3	26.7 ± 6.4

Table 2 Characterization of activation of $hNa_v1.7$ mutants in the presence of 100 nM HWTX-IV. Cells were held at -100 mV. Families of currents were induced by 50-ms depolarizing steps to various potentials ranging from -80 to +40 mV. Recording currents from WT and mutant $Na_v1.7$ started at ~20 min after establishing whole cell configuration. Note that the asterisk indicates that the concentration of HWTX-IV was 10 μM. All data come from 3-4 cells. The half-activation potential ($V_{1/2}$) and slope factor (*k*) were determined with Boltzmann fits. IC_{50} values were determined with Hill equation in Fig. 2B, in which slope factor was set to 1. The f_{bottom} values yielded were 0 on both wild type and mutant $Na_v1.7$ channels and therefore are not listed.

Figure 1

Molecular Pharmacology Fast Forward. Published on September 20, 2010 as DOI: 10.1124/mol.110.066332
This article has not been copyedited and formatted. The final version may differ from this version.

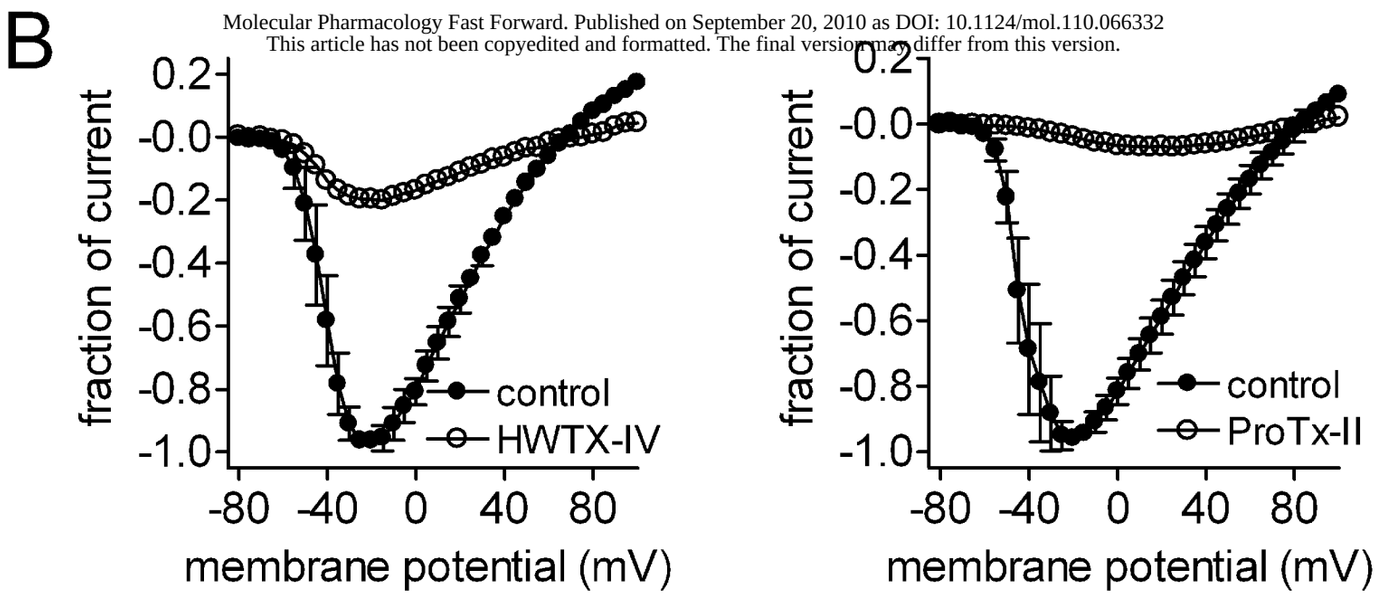

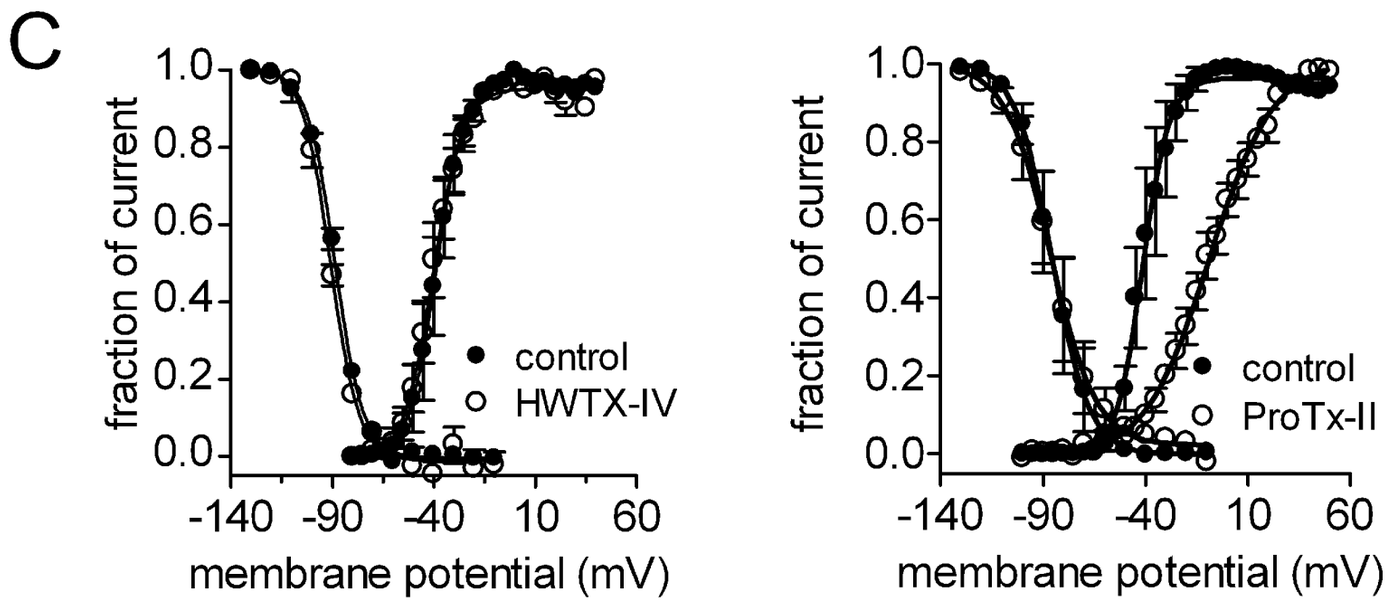

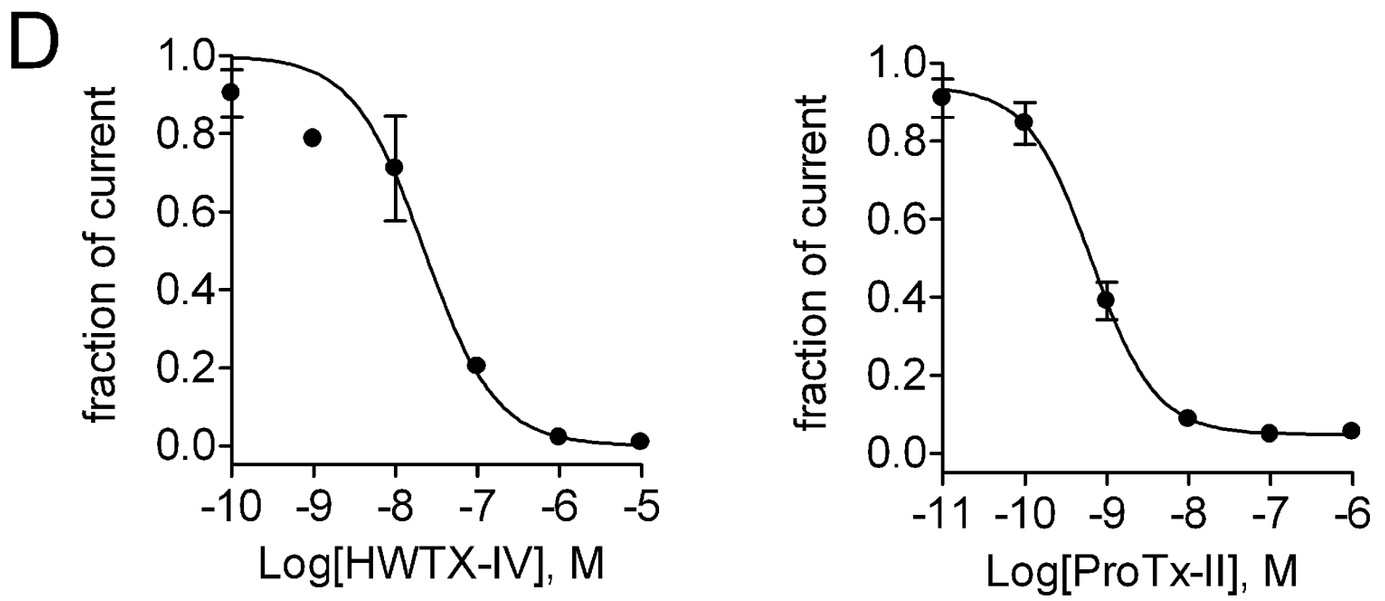

Figure 2

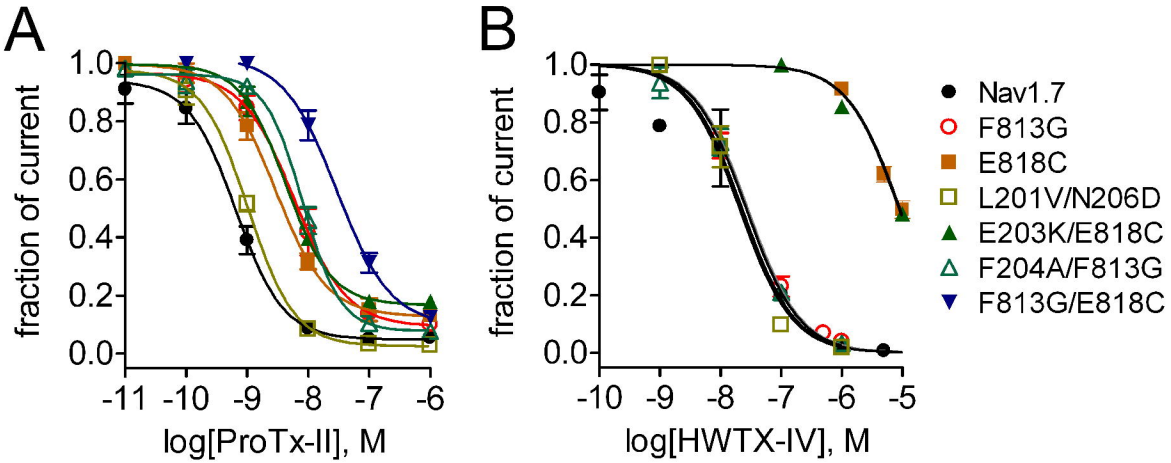
A
B
fraction of current
1.0
0.8
0.6
0.4
0.2
0.0
-11 -10 -9 -8 -7 -6
log[ProTx-II], M
-10 -9 -8 -7 -6 -5
log[HWTX-IV], M
Nav1.7
F813G
E818C
L201V/N206D
E203K/E818C
F204A/F813G
F813G/E818C

Figure 3

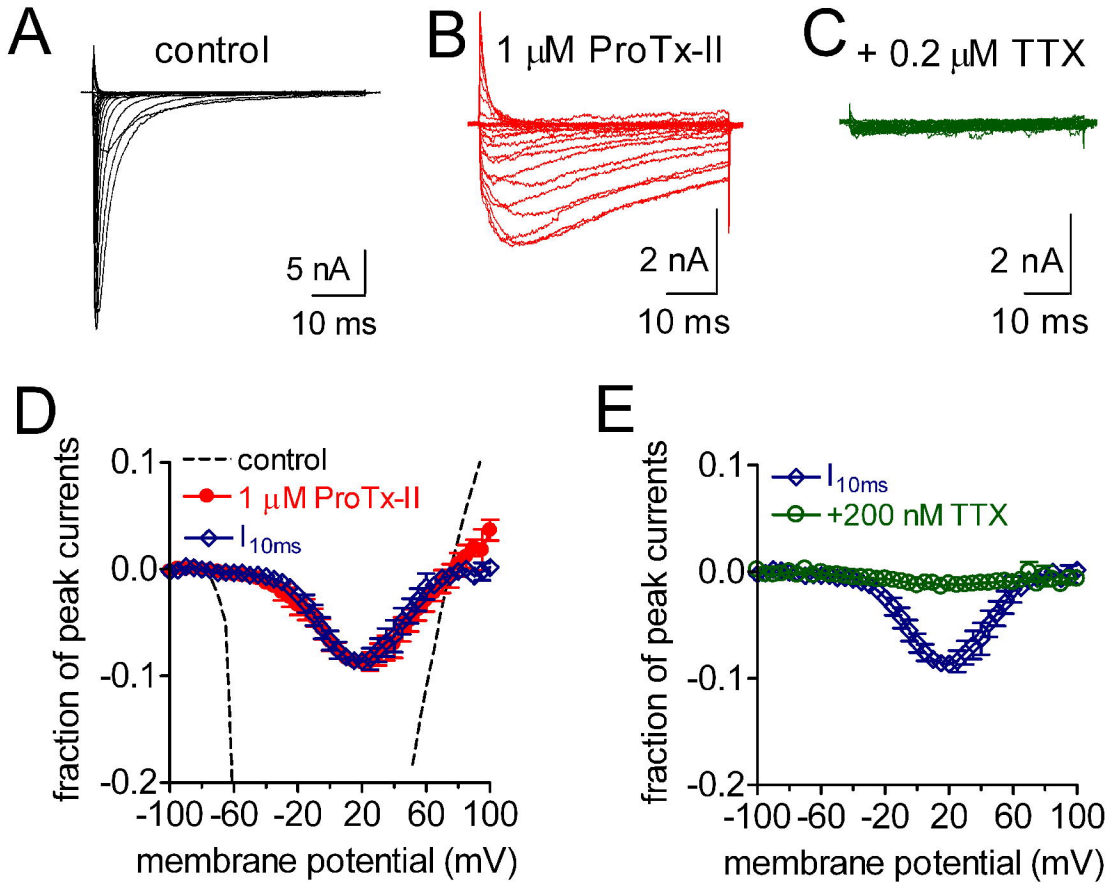
A
control
5 nA
10 ms
B
1 μM ProTx-II
2 nA
10 ms
C
+ 0.2 μM TTX
2 nA
10 ms
D
control
1 μM ProTx-II
I10ms
fraction of peak currents
0.1
0.0
-0.1
-0.2
-100 -60 -20 20 60 100
membrane potential (mV)
E
I10ms
+200 nM TTX
fraction of peak currents
0.1
0.0
-0.1
-0.2
-100 -60 -20 20 60 100
membrane potential (mV)

Figure 4

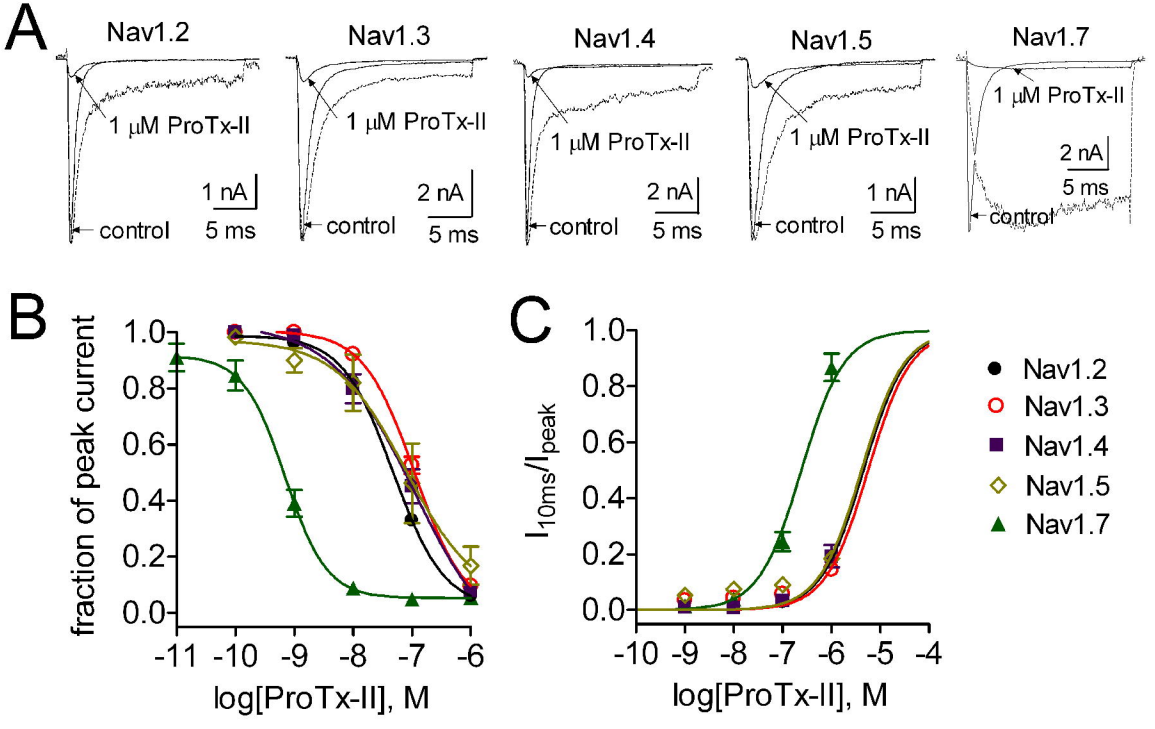
A
Nav1.2
1 μM ProTx-II
control
1 nA
5 ms
Nav1.3
1 μM ProTx-II
control
2 nA
5 ms
Nav1.4
1 μM ProTx-II
control
2 nA
5 ms
Nav1.5
1 μM ProTx-II
control
1 nA
5 ms
Nav1.7
1 μM ProTx-II
2 nA
5 ms
control
B
fraction of peak current
1.0
0.8
0.6
0.4
0.2
0.0
-11 -10 -9 -8 -7 -6
log[ProTx-II], M
C
I_{10ms}/I_{peak}
1.0
0.8
0.6
0.4
0.2
0.0
-10 -9 -8 -7 -6 -5 -4
log[ProTx-II], M
Nav1.2
Nav1.3
Nav1.4
Nav1.5
Nav1.7

Figure 5

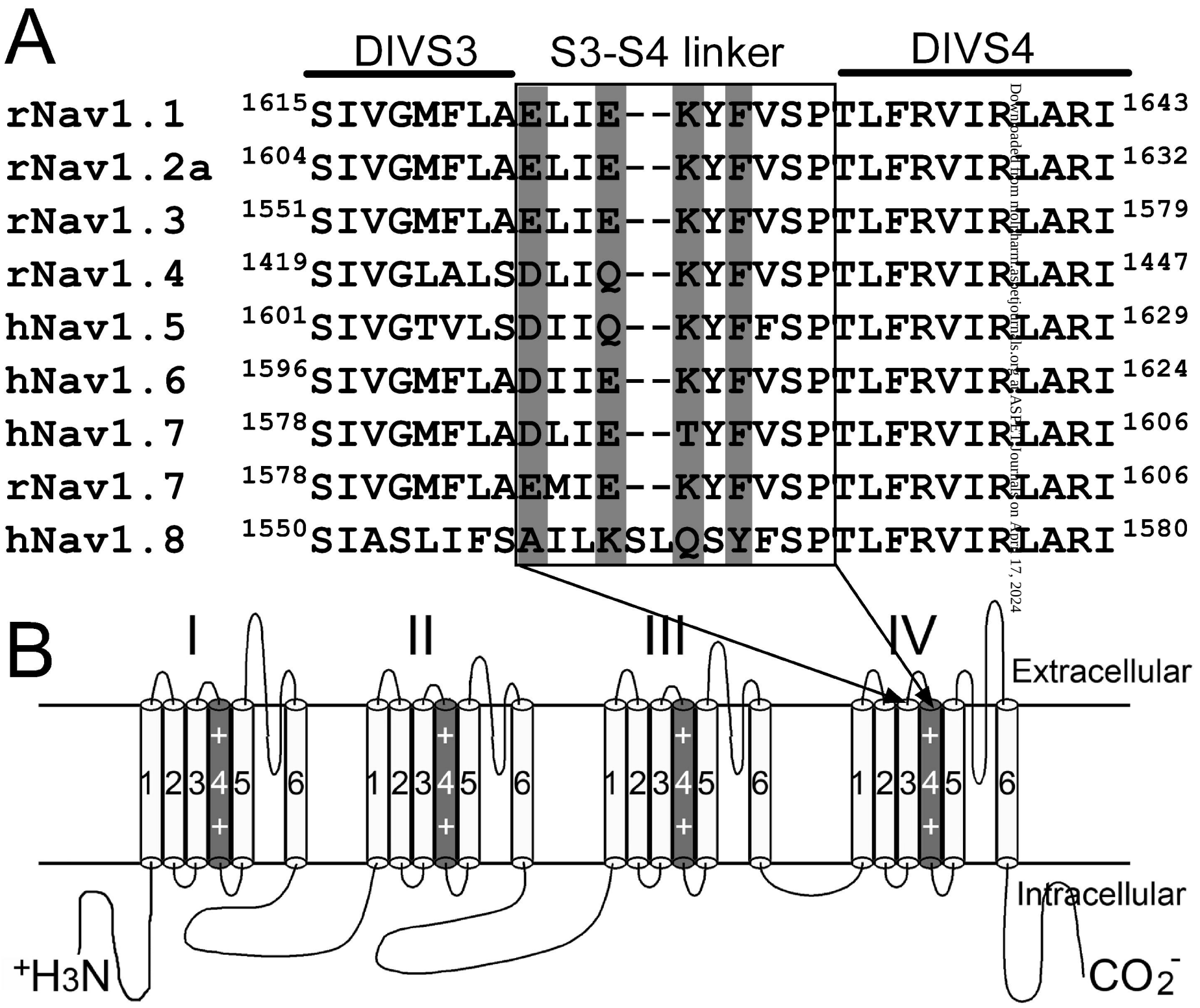

Figure 6

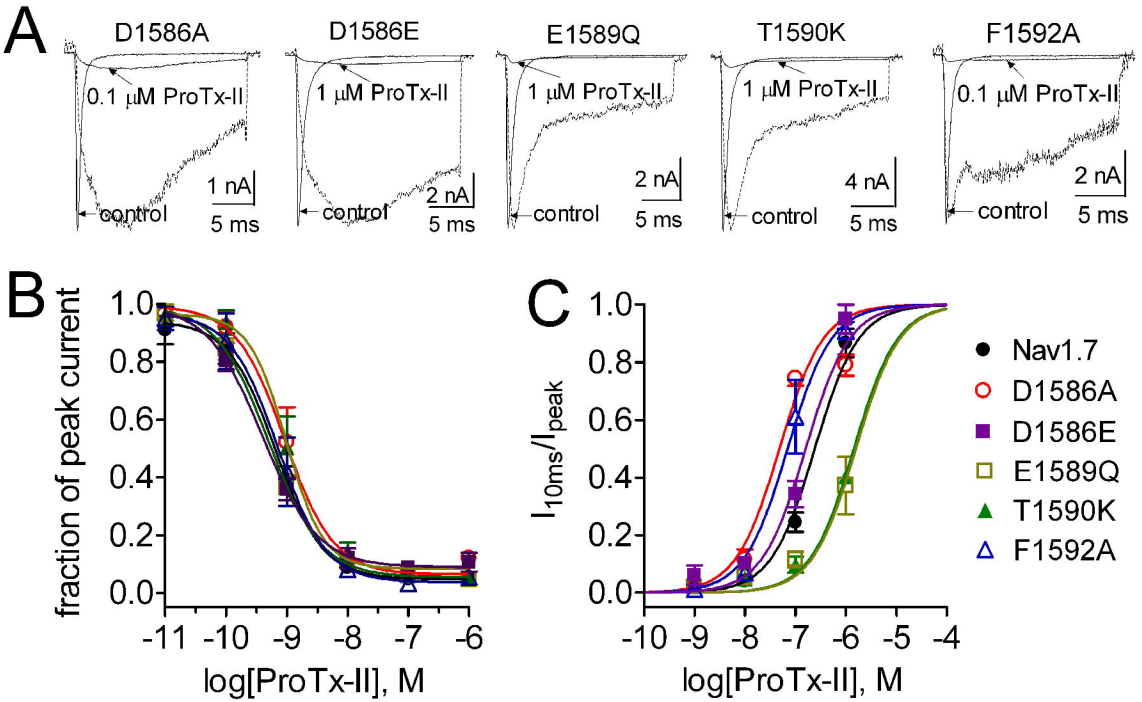
A
D1586A
0.1 μM ProTx-II
control
1 nA
5 ms
D1586E
1 μM ProTx-II
control
2 nA
5 ms
E1589Q
1 μM ProTx-II
control
2 nA
5 ms
T1590K
1 μM ProTx-II
control
4 nA
5 ms
F1592A
0.1 μM ProTx-II
control
2 nA
5 ms
B
fraction of peak current
1.0
0.8
0.6
0.4
0.2
0.0
-11 -10 -9 -8 -7 -6
log[ProTx-II], M
C
I10ms/Ipeak
1.0
0.8
0.6
0.4
0.2
0.0
-10 -9 -8 -7 -6 -5 -4
log[ProTx-II], M
Nav1.7
D1586A
D1586E
E1589Q
T1590K
F1592A

Figure 7

Molecular Pharmacology Fast Forward. Published on September 20, 2010 as DOI: 10.1124/mol.110.066332
This article has not been copyedited and formatted. The final version may differ from this version.

A

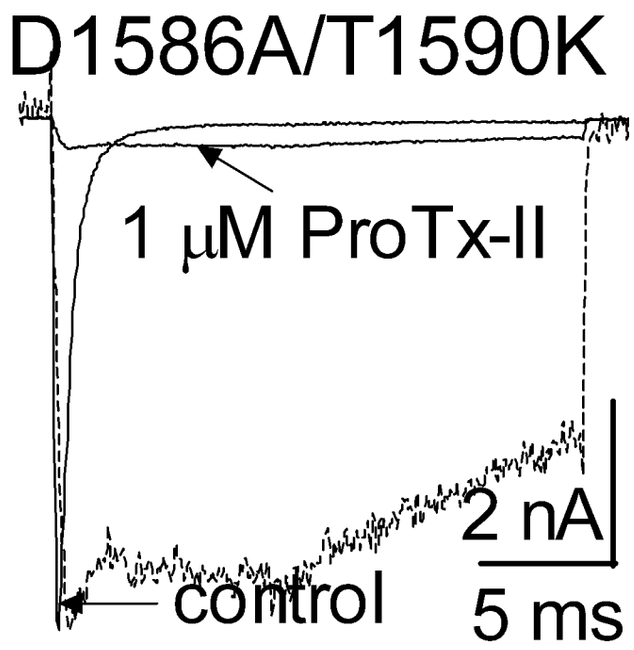

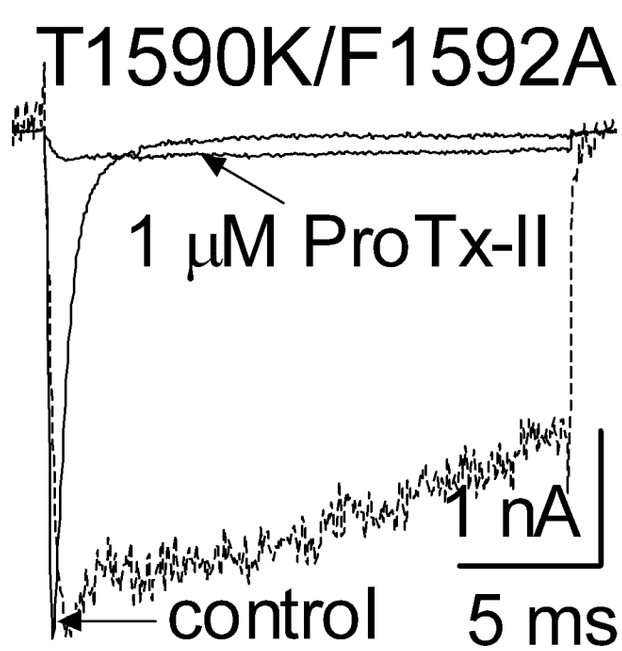

B

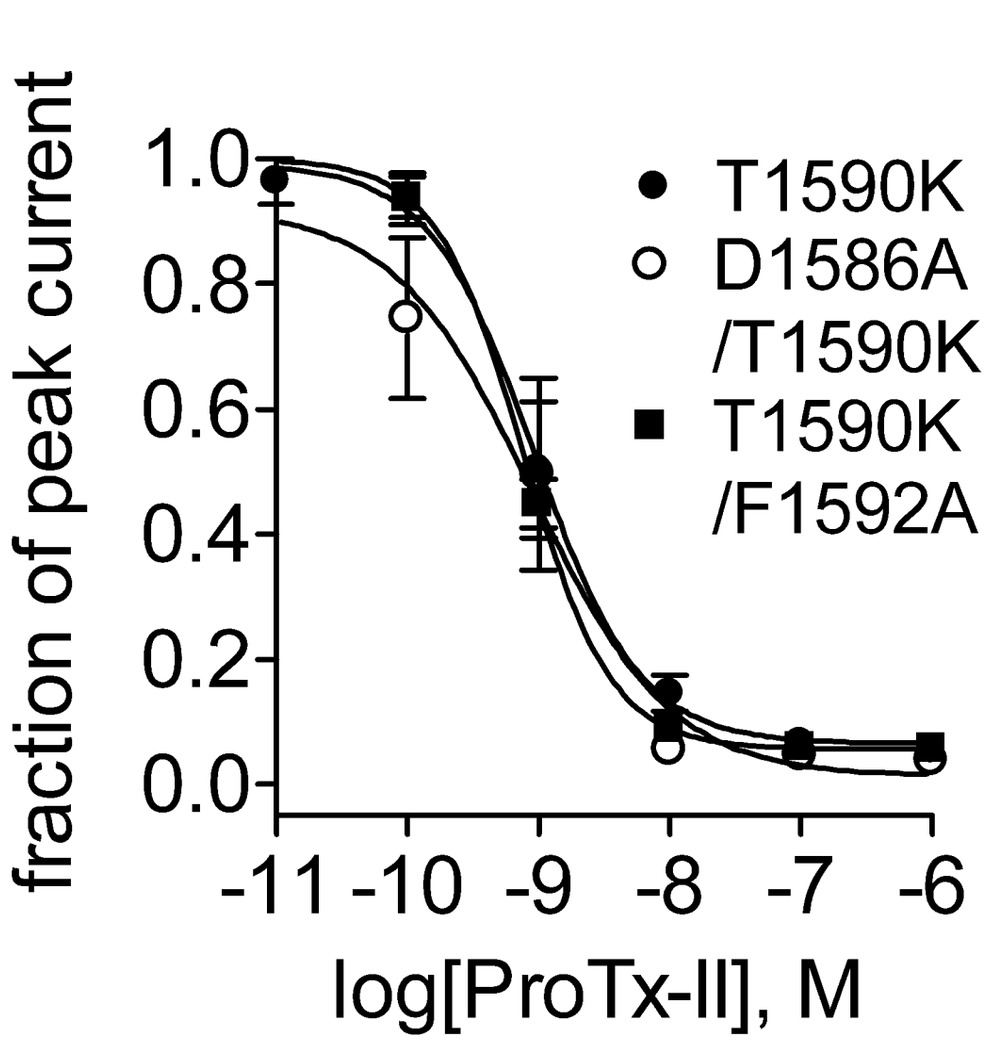

C

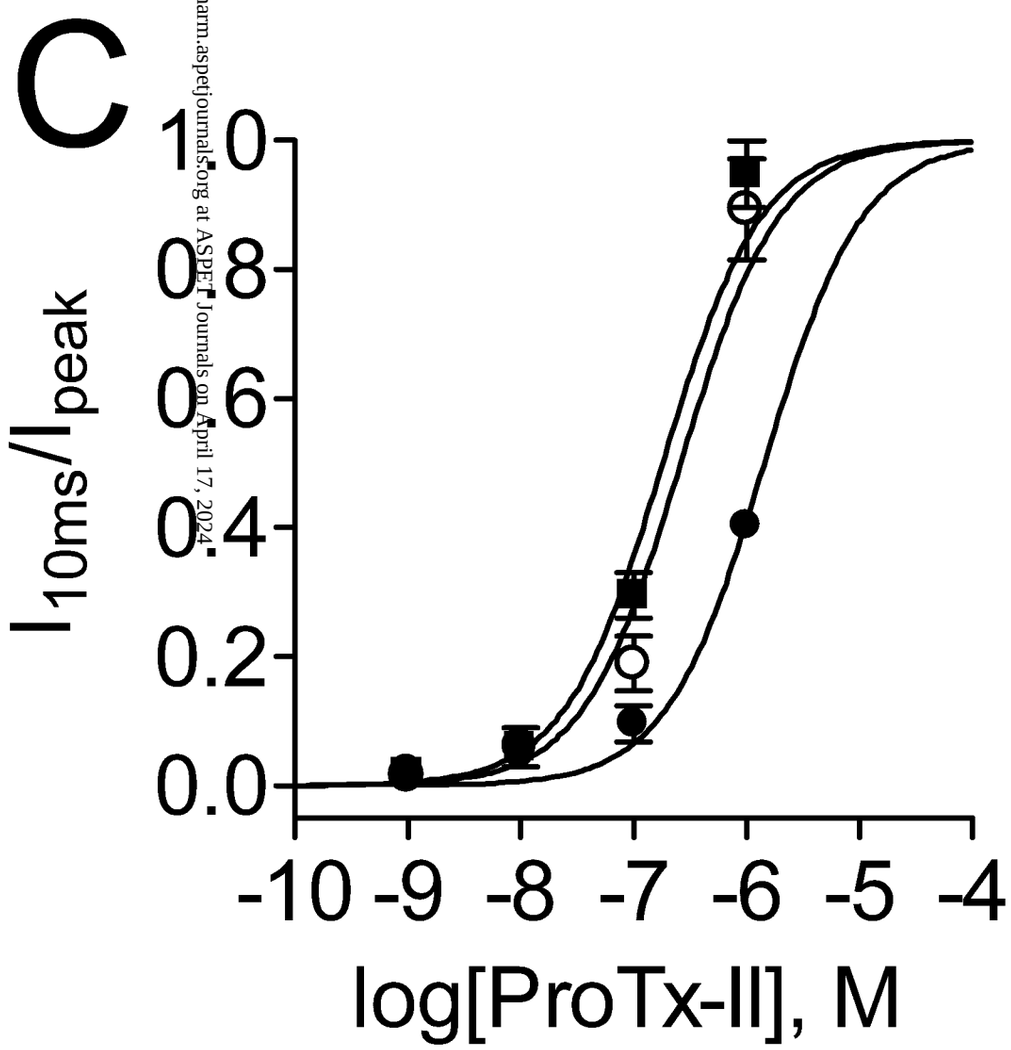

Supplemental Data

The tarantula toxins ProTx-II and HWTX-IV differentially interact with human Nav1.7 voltage-sensors to inhibit channel activation and inactivation

Yucheng Xiao, Kenneth Blumenthal, James O. Jackson II, Songping Liang and Theodore R. Cummins

Molecular Pharmacology

Supplemental Table S1.

Electrophysiological parameters of the voltage-dependence of steady-state activation and inactivation curves for wild type and mutant Nav1.7 channels. Cells were held at -100 mV. Families of currents were induced by 50-ms depolarizing steps to various potential ranging from -80 to +40 mV. Recording currents from WT and mutant Nav1.7 started at 5 min after establishing whole cell configuration. The voltage dependence of steady-state inactivation was estimated using a standard double-pulse protocol, in which a 20-ms depolarizing test potential of 0 mV followed a 500-ms prepulse at potentials that ranged from -130 to -10 mV with a 10-mV increment. Data points are shown as mean ± S.E. The half-activation potential ($V_{1/2}$) and slope factor (k) were determined with Boltzmann fits.

Channel	Voltage dependence of activation			Voltage dependence of inactivation		
	$V_{1/2}$, mV	k, mV	n	$V_{1/2}$, mV	k, mV	n
hNav1.7	-28.0 ± 0.6	7.7 ± 0.5	11	-80.1 ± 1.0	7.6 ± 0.6	12
L201V/N206D	-29.0 ± 0.5	7.2 ± 0.5	9	-81.2 ± 0.6	7.4 ± 0.6	9
F813G	-24.5 ± 0.4	7.7 ± 0.4	14	-76.3 ± 0.6	7.6 ± 0.5	12
E818C	-20.2 ± 0.3	7.6 ± 0.3	10	-77.1 ± 0.5	6.4 ± 0.4	7
E203K/E818C	-10.4 ± 0.2	8.9 ± 0.2	11	-75.7 ± 0.5	6.6 ± 0.5	8
F204A/F813G	-23.0 ± 0.6	7.6 ± 0.5	7	-81.2 ± 0.6	7.4 ± 0.6	6
F813G/E818C	-18.8 ± 0.5	8.3 ± 0.5	8	-77.5 ± 0.6	7.7 ± 0.6	7
D1586A	-26.1 ± 0.6	7.5 ± 0.6	7	-83.1 ± 0.3	6.6 ± 0.2	7
D1586E	-25.6 ± 0.4	6.8 ± 0.3	7	-80.6 ± 0.6	6.9 ± 0.6	7
E1589Q	-23.0 ± 0.4	7.0 ± 0.3	8	-75.2 ± 0.6	7.0 ± 0.5	9
T1590K	-23.9 ± 0.3	6.7 ± 0.3	9	-77.4 ± 0.5	7.5 ± 0.4	9
F1592A	-24.7 ± 0.5	7.3 ± 0.4	7	-85.5 ± 0.4	6.6 ± 0.3	6
D1586A/T1590K	-25.3 ± 0.4	6.8 ± 0.3	6	-84.7 ± 0.4	7.6 ± 0.4	6
T1590K/F1592A	-19.8 ± 0.5	7.9 ± 0.5	4	-82.7 ± 1.0	8.6 ± 0.9	4

Supplemental Table S2.

IC50 values for ProTx-II slowing fast-inactivation of WT sodium channel isoforms and mutant hNav1.7 channels. IC_{50} values were determined with Hill equation in Fig. 4C, Fig. 6C and Fig. 7C, in which the slope factor (*nH*) was set to 1 because only sodium channel DIV is involved in channel inactivation gating.

Channel	IC_{50}, μM	Nav1.7 mutants	IC_{50}, μM
Nav1.2a	4.5 ± 0.3	D1586A	0.05 ± 0.02
Nav1.3	5.6 ± 0.5	D1586E	0.16 ± 0.02
Nav1.4	4.2 ± 0.4	E1589Q	1.6 ± 0.8
Nav1.5	4.1 ± 0.3	T1590K	1.4 ± 0.3
Nav1.7	0.25 ± 0.04	F1592A	0.07 ± 0.01
		D1586A/T1590K	0.26 ± 0.04
		T1590K/F1592A	0.18 ± 0.02

Supplemental Fig. S1. Sequence alignment of DIS3-S4 linker on sodium channel isoforms. The isoforms Nav1.1, Nav1.2a, Nav1.3 and Nav1.4 are from rats while the others are from human. In (A), two conserved residues of interest are shaded in grey. In (B), two divergent residues in hNav1.7 splice variant hNav1.7a are shaded in grey. (C) Schematic showing position of mutations studied in domains I and II.

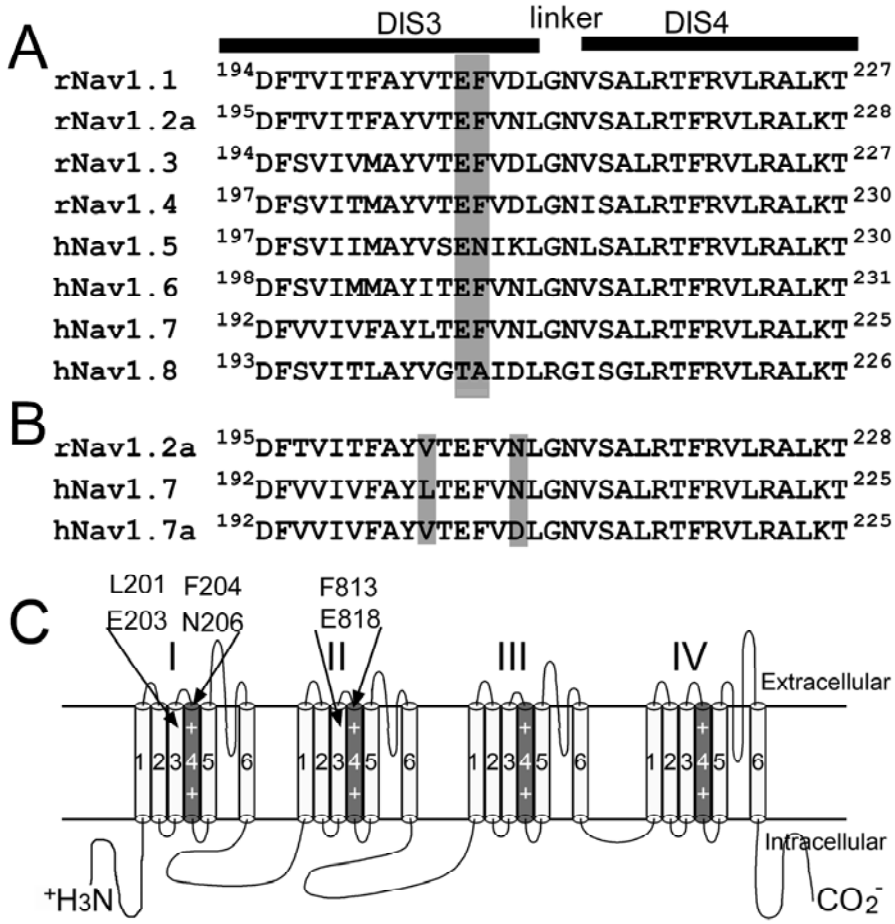

Supplemental Fig. S2. HWTX-IV did not slow fast-inactivation of wild type (A) and mutant E818C (B) hNav1.7 channels. Current traces were elicited by a 20-ms depolarization of -10 mV from a holding potential of -100 mV. Toxin concentrations were 1 μM for wild type hNav1.7 and 10 μM for mutant E818C hNav1.7.

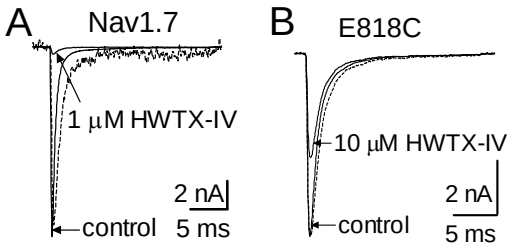

Supplemental Fig. S3. Sequence alignment of DIIS3-S4 linkers of eight sodium channel isoforms. The isoforms Nav1.1, Nav1.2, Nav1.3 and Nav1.4 are from rat while the others are from human. The residues that are crucial for binding to ProTx-II and HWTX-IV are shaded in grey.

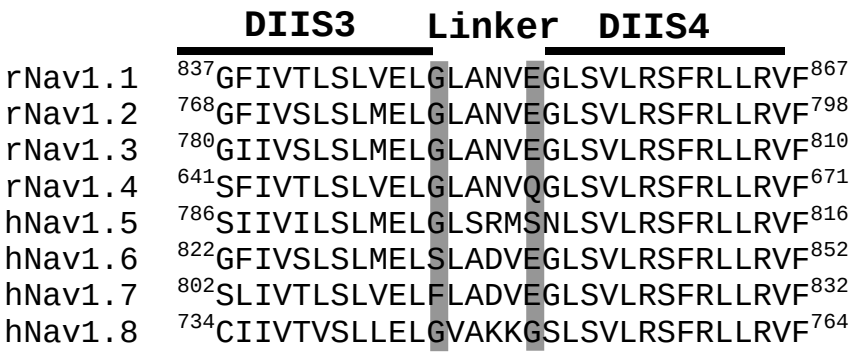

Supplemental Fig. S4. Mutations in DIV S3-S4 linker differentially alter fast-inactivation of hNa$_v$1.7 channels expressed in HEK293 cells. Representative current traces for five mutant (D1586A, D1586E, E1589Q, T1590K and F1592A) and WT hNa$_v$1.7 channels. The test pulse potential was -10 mV (WT hNa$_v$1.7, D1586A and D1586E) and -5 mV (E1589Q, T1590K and F1592A), respectively. Cells were held at -100 mV. The currents are shown before and after application of 0.1 or 1 μM ProTx-II, and are magnified to focus on the sustained components. Note that under control conditions hNa$_v$1.7 channels produce negligible amounts of sustained currents.

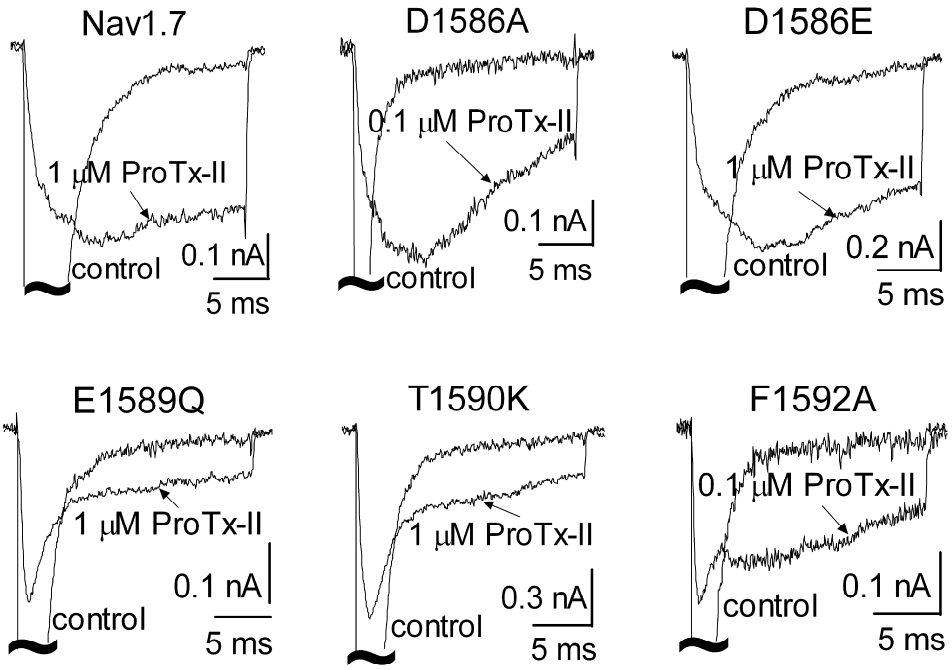

Supplemental Fig. S5. Mutations in DIV S3-S4 linker differentially alter the effect of ProTx-II on fast-inactivation of hNa$_v$1.7-F813G/E818C double mutant channels expressed in HEK293 cells. (A) Representative current traces for F813G/E818C, F813G/E818C/E1589Q and F813G/E818C/F1592A channels before and after exposure to ProTx-II. The test pulse potential was 0 mV. Cells were held at -100 mV. The dotted line shows the residual current in the presence of 1 μM ProTx-II after normalization to the maximum amplitude of control current. (B), Concentration-dependent inhibitory curves of ProTx-II on the activation of three mutant (F813G/E818C, F813G/E818C/E1589Q and F813G/E818C/F1592A) hNav1.7 channels. The residual current after toxin treatment was plotted as fraction of the control current. Data points (mean ± S.E., each from 3 - 6 cells) were fit with a Hill equation as described under "Experimental Procedures". Their apperant IC_{50} values are 29.8, 24.6 and 26.5 nM, respectively. (C), Concentration-dependent inhibitory curves of ProTx-II on the fast-inactivation of three mutant (F813G/E818C, F813G/E818C/E1589Q and F813G/E818C/F1592A) hNav1.7 channels. The I_{10ms} value was plotted as a fraction of the residual current after ProTx-II treatment. Data points (mean ± S.E., each from 3-6 cells) were fitted with Hill equation as described under "Experimental Procedure". The apparent IC_{50} values are estimated to be 0.87, 4.38 and 0.11 μM, respectively.